

# Jurassic and Cretaceous foreland basin deposits of the Russian Arctic: Separated by birth of the Makarov Basin?

Elizabeth L. Miller, Alex Soloviev, Alexander Kuzmichev, George Gehrels,  
Jaime Toro & Marianna Tuchkova

KuMiller, E.L., Soloviev, A., Kuzmichev, A., Gehrels, G., Toro, J. & Tuchkova, M.: Jurassic and Cretaceous foreland basin deposits of the Russian Arctic: Separated by birth of the Makarov Basin? *Norwegian Journal of Geology*, Vol. 88, pp. 201-226. Trondheim 2008. ISSN 029-196X.

The age and mode of formation of the various sub-basins of the Amerasian Basin of the Arctic Ocean remain unknown. Jurassic-Cretaceous syn-orogenic foreland basin deposits are the youngest stratigraphic units deposited in the Russian Arctic prior to rifting and formation of the Amerasian Basin. U-Pb dating of detrital zircon suites (6 samples, ~ 100 zircons each) by LA-ICP-MS reveal that sandstones in the New Siberian Islands have nearly identical sources to those in Chukotka and the South Anyui Zone (SAZ) despite evidence for proximal derivation and little transport. These include abundant Precambrian (~2.1-1.7 Ga), Late Paleozoic (~330-250 Ma) and lesser Mesozoic (~175 to 145 Ma) ages; youngest zircons are likely derived from Main Belt granites in the N. Verkoyansk. The foreland basin and its counterpart the orogenic highlands either extended continuously for ~1400 km along strike, or the localities studied were once much closer together. We hypothesize that rifting/extension associated with formation of the Makarov Basin and development of the SAZ as a transform fault might be one way of explaining the present separation of the study sites

Elizabeth L. Miller, Department of Geological and Environmental Sciences, Stanford University, Bld. 320, Stanford, CA, 94305, USA, miller@pangea.stanford.edu; Alex Soloviev, Alexander Kuzmichev & Marianna Tuchkova, Geological Institute, Russian Academy of Sciences, Pyzhevsky 7, Moscow 119017, Russian Federation, solov@ilran.ru; George Gehrels, Department of Geosciences, University of Arizona, Tucson, AZ, 85721, USA, ggehrels@geo.arizona.edu; Jaime Toro, Department of Geology and Geography, West Virginia University, WV, 26506, USA, jtoro@wvu.edu

## Introduction

The age of rifting and the mode of formation of the Amerasian Basin of the Arctic have far-reaching implications for the origin of its broad continental shelves, their oil and gas potential, the role the Arctic Ocean has played in global climate, and, most recently, for claims to extend outer continental shelf limits under Article 76 of UNCLOS (e.g., Macnab 2006). Despite the fact that the plate tectonic origin of the Amerasian Basin has been cited as a top research priority by numerous international working groups, logistics and cost continue to preclude scientific drilling of its seafloor. The Gakkel Ridge in the Eurasian Basin is the northern continuation of the mid-Atlantic Ridge (Fig. 1A). Restoration of its Cenozoic spreading history places the Lomonosov Ridge, a strip of continental crust, against the Barents Shelf (e.g., Rowley & Lottes 1988) (Fig. 1B), leaving the older and more controversial Amerasian Basin to be explained by other rift mechanisms (Fig. 1A,B). The Amerasian Basin consists of the Makarov Basin, the Alpha and Mendeleev Ridges, and the Canada Basin (Fig. 1A). The origin of these basins and intervening highs have been debated for years (e.g. review in Lawver & Scotese 1990). Grantz et al. (1979) proposed a rotational opening model for the Amerasian Basin where the Lomonosov margin of the Amerasian Basin operates

as a strike-slip or transform fault boundary, a model which remains the most cited today. In the rotational rift model, the Alpha and Mendeleev Ridges must be parts of a younger feature, perhaps a hot spot related volcanic edifice (e.g., Lawver et al. 2002). Previous interpretations of the Makarov Basin included one which interpreted it as a Late Cretaceous oceanic basin that formed parallel to the Lomonosov Ridge by rift opening in a direction orthogonal to the Lomonosov Ridge based on magnetic anomalies (e.g. Sweeney et al. 1982; Taylor et al. 1981; Vogt et al. 1982). In this model, the Alpha and Mendeleev Ridges with their subparallel basins and highs (Fig. 1A) might represent a component of what was rifted away from the Lomonosov Ridge. More recent magnetic data (Glebovsky et al. 2000) do not reveal the earlier interpreted anomalies, and seismic refraction studies show that the Mendeleev Ridge is underlain by thick (~ 34 Km) but mostly mafic (6.8- 7.6 km/sec) crust (e.g., Ivanova et al. 2006). A detailed analysis of the Lomonosov Ridge by Cochran et al. (2006) argues in favor of the Grantz et al. (1979) model. Thus the “rotational rift” model is the most agreed upon model for the formation of the Amerasian Basin. This model makes several specific predictions for the Russian Arctic. The rotational rift model argues that the Arctic Alaska-Chukotka microplate (AACM) rotated from the Canadian Arctic margin to where it is today in Arctic Russia, closing an ocean basin,

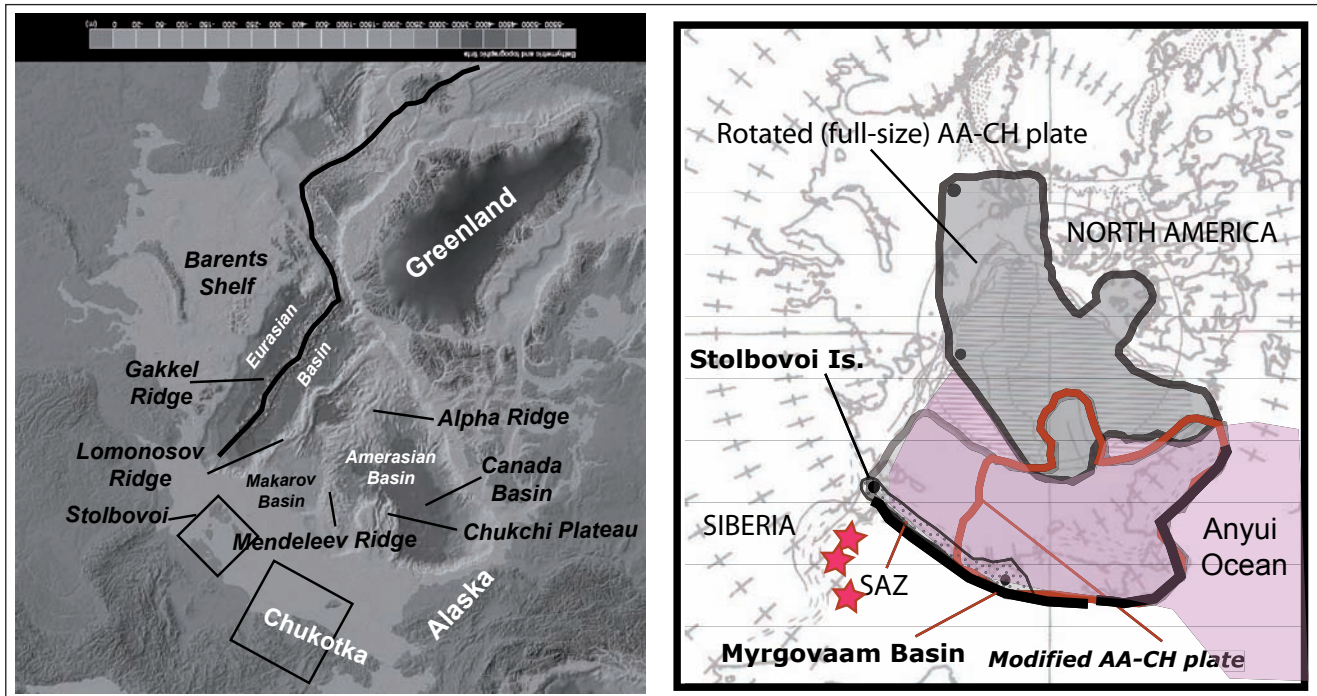


Figure 1. A. Index and bathymetry of the Arctic Ocean (IBCAO, 2002) showing location of the Amerasian Basin and its features. Boxes show the approximate locations of Figures 2 (New Siberian Islands) and 3 (Chukotka). B. Schematic diagram showing the proposed size and shape(s) of the Arctic Alaska-Chukotka plate and its inferred restored position along the Canadian Arctic margin prior to rotational rift opening of the Amerasian Basin. Light shaded region (pink) is the location of the inferred Anyui Ocean that once lay between Siberia and North America. Basemap of Figure 1B is from Rowley & Lottes (1988) and shows the Eurasian or North Atlantic basin closed at 140 Ma. Sandstones we compare in this paper are shown at opposite ends of a hypothetical foreland basin, the Myrgovaam (Rauchua) Basin. The South Anyui Zone (SAZ) is shown by a black line that continues into Alaska as the Angayucham zone, and is characterized by remnants of oceanic and island arc terranes. Red stars are loci of Main Belt granitoid plutons studied and dated by Toro et al. (2007), Prokopiev et al. (2007) and Akinin et al. (in press).

the “Anyui Ocean” south of the rotating plate (Fig. 1B) (e.g., Grantz et al. 1979; Grantz & May 1982; Rowley & Lottes 1988; Grantz et al. 1990; Lavwer et al. 2002). The time interval of rotation is 135–120 Ma (Fig. 1B) (Lavwer et al. 2002). Rowley & Lottes (1988) discuss another key geologic aspect of the rotation model: It is viable only if the Arctic Alaska-Chukotka microplate (AACM) is the right shape and size so that it doesn’t significantly overlap the Lomonosov Ridge and (once) adjacent Barents Shelf in the process (Fig. 1B). Thus, supporters of the rotation model draw the western end of the rotating plate at some arbitrary position in the Russian Arctic that allows for a better fit (e.g., Rowley & Lottes 1988; Grantz et al. 1979; Grantz & May 1982; Lavwer et al. 2002; Kuzmichev 2009) (Fig. 1B). Problems presented by the rotational opening model for Arctic Russia include the fact that geologists have long cited evidence that the southern boundary of the AACM, the South Anyui suture zone (SAZ) extends to the New Siberian Islands (e.g. Parfenov & Natali’ in 1985; Fujita & Cook 2000; Kuzmichev et al. 2006; Kuzmichev 2009), making the plate too big to fit the rotation model (Fig. 1). More recently, detrital zircon geochronology of Triassic strata from the margins of the Amerasian Basin provided a very preliminary data set to evaluate this model (Miller et al. 2006). This new data suggested that Chukotka has greater affinity with NE Russia instead of the Canadian margin.

This paper directly addresses the question of the paleogeographic origin of Chukotka, the extent of the AACM and the timing of its deformational events by comparing the tectonic setting, petrography and single-grain U-Pb ages of detrital zircons of Volgian or Tithonian to Valanginian (Late Jurassic to Early Cretaceous) syn-orogenic foreland basin sandstones in two distant parts of the AACM, Stolbovoi Island, (New Siberian Islands) and central Chukotka and the South Anyui Zone (SAZ) (mainland Arctic Russia), localities that are now ~ 1400 km apart (Fig. 1). The syn-orogenic sandstones are derived from collision or shortening-related orogenic highlands that lay to the south of the SAZ. Foreland basin sediments were shed northward across platformal sequences that underlie the northern part of the New Siberian Island Archipelago and across an actively deforming region of the Chukotka fold belt in Chukotka. Their remarkable similarity in the two regions provides new data with which to constrain plate models for the Amerasian Basin of the Arctic.

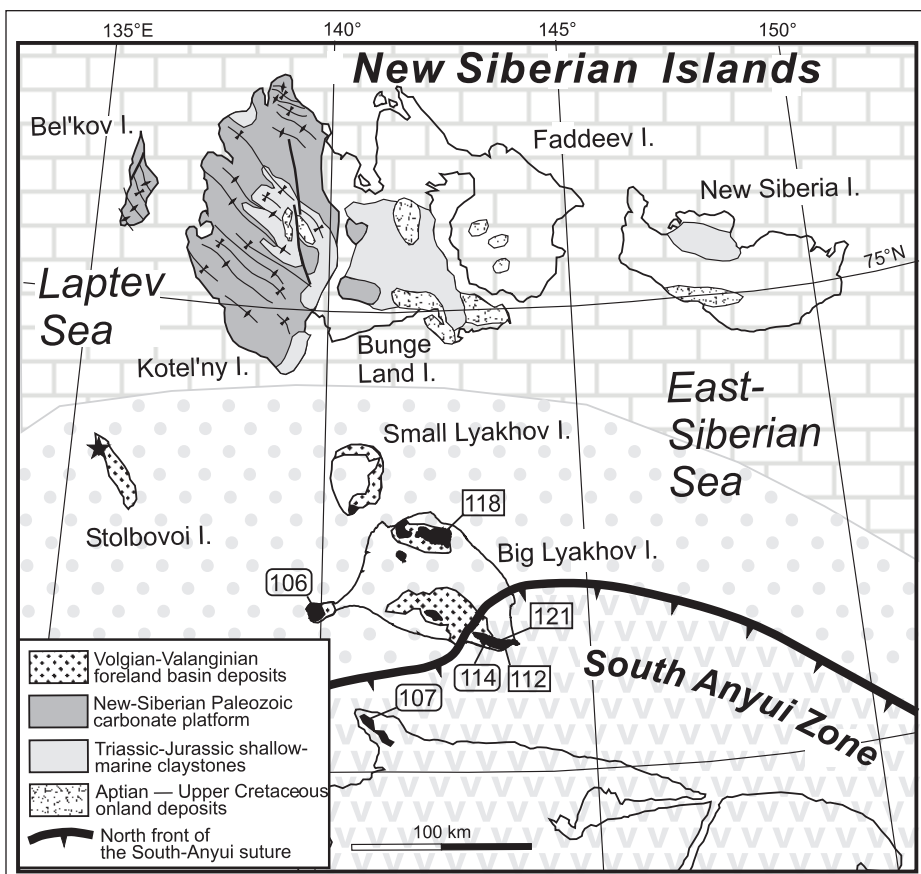
## Regional geology

Deformation of Paleozoic and Mesozoic sequences of the AACM and closure of the Anyui oceanic basin along its southern edge led to the deposition of the

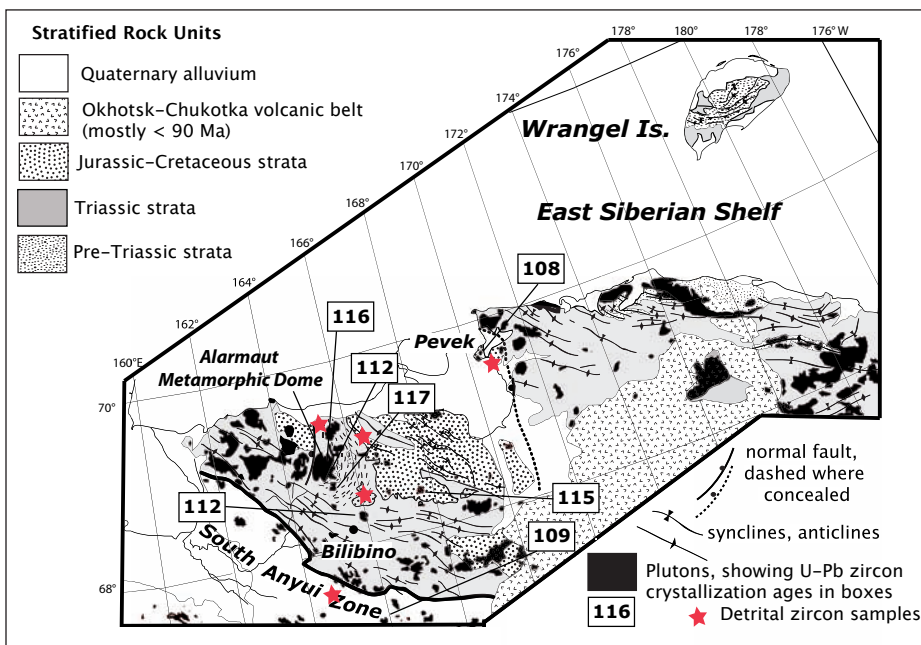
Jurassic-Cretaceous syn-orogenic foreland basin sequences described here. This deformation has been recently studied on Stolbovoi and Big Lyakhov Islands by Kuzmichev et al. (2006) and Kuzmichev (2009), in Chukotka by Katkov et al. (2006), Miller et al. (in press) and Miller & Verzhbitsky (in press), and in the SAZ by Sokolov et al. (2002) and Bondarenko et al. (2003) (Figs. 2 and 3). In these localities, deformation has been linked

to crustal shortening and arc collision and lesser strike-slip faulting (Sokolov et al. 2002). As described by these authors, deformation was accompanied by uplift which led to the deposition of southerly-derived, northerly-transported synorogenic clastic sequences. These clastic sequences are mostly basinal gravity flow deposits derived from mixed sources that include deformed platform to basinal Paleozoic-Mesozoic sequences, coarse

**Figure 2.** Simplified geologic and tectonic map of the New Siberian Islands and the South Anyui Suture Zone (SAZ) after Vol'nov et al. (1998) and Kuzmichev et al. (2005, 2006). Black star is location of sample analyzed for detrital zircons in this study (for exact location see Table 2). Light grey patterns outline the extent of allochthonous arc and oceanic rocks ( $v$  pattern), Tithonian to Valanginian syn-orogenic basin deposits (dots) and platformal rocks (limestone pattern). Age of granitic rocks is from Layer et al. (2001), Dorochev et al. (2001) and unpublished data of Kuzmichev. Rounded rectangles are  $^{40}\text{Ar}/^{39}\text{Ar}$  biotite plateau ages and rectangles are U-Pb zircon ages.



**Figure 3.** Simplified geologic and tectonic map of Chukotka showing the Anyui-Chukotka fold belt, the distribution of Jurassic-Cretaceous syn-orogenic deposits and the younger (syn-extensional) plutons that intrude the fold belt (with U-Pb ages in squares), after Miller and Verzhbitsky (in press). Stars are locations of detrital zircon samples (for exact localities see Table 2).



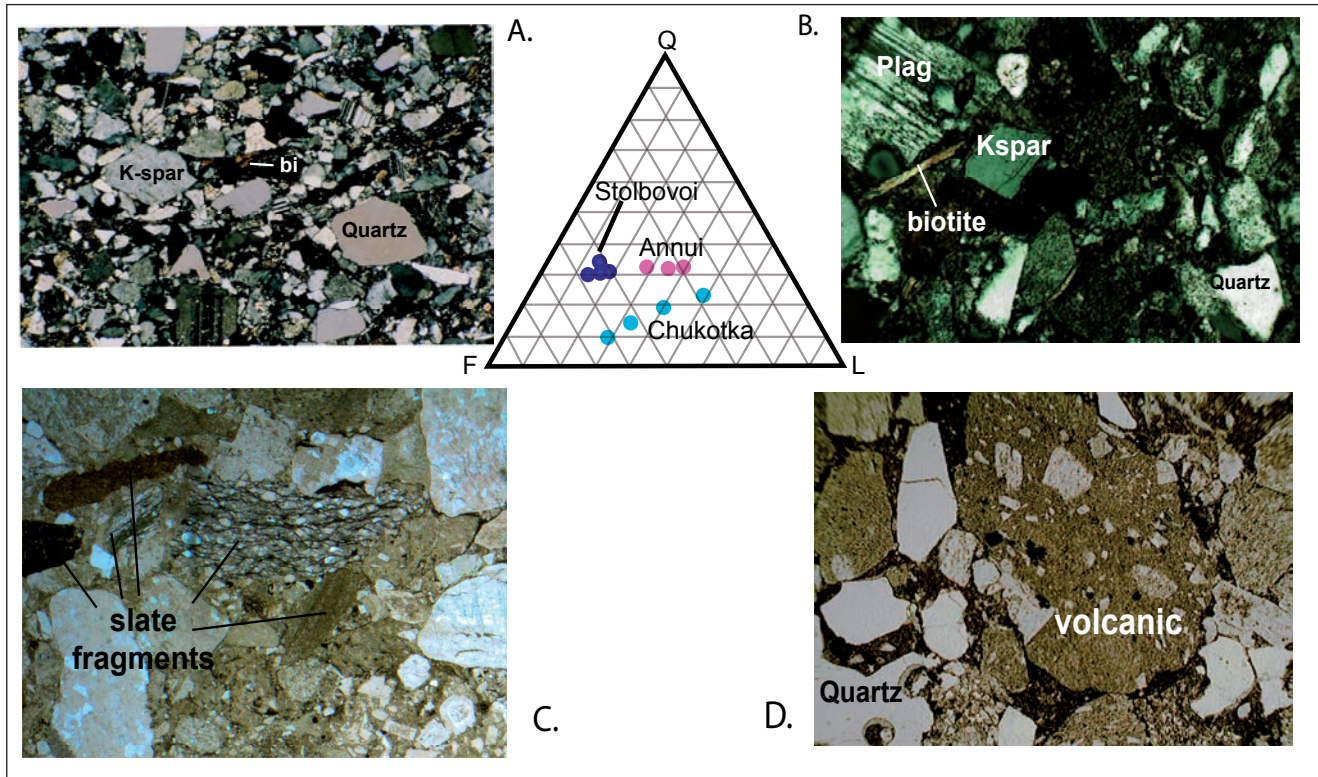


Figure 4. Point-count data and photomicrographs of Jurassic-Cretaceous samples. A. Sample ELMCH03.24.3, x-polars, field of view ~ 3mm. Note abundance of angular plagioclase, K-feldspar, monocrystalline quartz and biotite. B. Sample 53.1 from Stolbovoi, x-polars, field of view ~ 1 mm. C. Jurassic-Cretaceous sandstone from Chukotka with abundant rock fragments of deformed slate (most likely from deformed Triassic and older strata), planar light, ~ 2mm across. D. Jurassic-Cretaceous from Chukotka with abundant volcanic detritus including monocrystalline embayed quartz phenocrysts from felsic volcanic sources, planar light, ~ 2mm across.

**Table 1. Sandstone petrography**

(Point count data from sandstones collected from J3-K1 deposit of Russian Arctic)

Sample	Q%	F%	L%	Mtx%	Lv	Ls	Lm
50/1-02 Stolbovoi	30.3	56.3	13.3	26.6	55.6	33.3	11.1
51/1-02 Stolbovoi	34.3	51.3	14.3	24.4	52.0	32.0	16.0
53/1-02 Stolbovoi	31.3	49.8	18.9	28.5	31.6	63.2	5.3
54/1-02 Stolbovoi	30.7	52.0	17.3	23.3	48.3	37.9	13.8
CH03ELM 24.3	9.35	61.94	28.75	0.92	82.02	12.36	5.6
CH04 JT54A	31.75	33.33	34.92	9	63.64	18.2	18.2
CH04 JT54D	14.8	52.8	32.4	4.2	67.9	19.75	12.35
CH04 ELM7	18.8	41.03	40.17	1.63	72.34	15.96	11.7
CH04 ELM23A	14.11	28.22	57.67	15	73.4	25.53	1.06
GB9986 SAZ	33.47	26.45	40.08	3.2	29.9	38.14	15.5
GB9947 SAZ	23.81	26.98	49.21	4.25	83.9	12.9	3.23
9947/1 SAZ	32.73	38.2	29.1	13.3	87.5	12.5	0

Notes: Q% = Q/ $\Sigma$ ; F% = F/ $\Sigma$ ; L% = (Lv + Ls + Lm + Col)/ $\Sigma$ ; Mtx% = Mtx/(Mtx +  $\Sigma$ ); Lv = Lv/(Lv + Ls + Lm),  
 $L_s = Ls/(Lv + Ls + Lm)$ ,  $L_m = Lm/(Lv + Ls + Lm)$  v - volcanic, s - sedimentary, m - metamorphic

crystalline rocks, and volcanic/plutonic rocks. In the New Siberian Islands, Jurassic-Cretaceous syn-orogenic strata are interpreted to have been deposited northwards from a region of allochthonous arc and ophiolitic rocks exposed on Big Lakhov Island and the Russian mainland (Kuzmichev et al. 2006) (Fig. 2). In Chukotka, the map distribution of Jurassic-Cretaceous strata extends at least as far south as the SAZ (Fig. 3), where deformed strata of this age underlie most of that zone. Despite the complex deformation in this zone, Jurassic-Cretaceous syn-orogenic sandstones are inferred to have been derived from the south (e.g., Sokolov et al. 2002; Bondarenko et al. 2003). The syn-orogenic sediments of Chukotka were deposited across the evolving Chukotka fold belt, and are in turn deformed as well. The northernmost exposures are found along the Arctic coast near the town of Pevk (Fig. 3), where they have much lower sand:shale ratios than strata further south. Sparse fossils from all of these localities indicate Late Jurassic to Early Cretaceous ages (Volgian or Tithonian to Valanginian (e.g. Samusin & Belousova 1985; Paraketsov & Paraketsova 1989), which, for the sake of convenience, we refer to as "Jurassic-Cretaceous" (J3-K1 in Russian literature). Within the SAZ proper, Dovgal (1964) describes strata with fossils as young as Hauterivian-Barremian that are involved in at least the latest stages of deformation (see also summary in Bondarenko et al. 2003). The deformed Jurassic-Cretaceous syn-orogenic deposits are intruded by post-tectonic plutons at least as old as 121 Ma in the New Siberian Islands (Fig. 2) (Layer et al. 2001; Dorofeev et al. 2001; Kuzmichev 2009) and at least as old as 116.9 ± 2.5 Ma in Chukotka (Fig. 3) (Katkov et al. 2007; Miller et al. in press). Quaternary deposits cover most of the topographically low coastal region of the Russian Arctic that lies between Chukotka and the New Siberian Islands (Fig. 1A), so there is no map continuity between any of the units exposed in these two distant locations.

## Sandstone description and petrography

### New Siberian Islands

The New Siberian Islands are represented mostly by a Paleozoic-Mesozoic platformal sequence (Kos'ko et al. 1985, 1990; Fujita & Cook 1990; Dorofeev et al. 1999) which, prior to opening of the Eurasian basin, was attached to the Siberian edge of the Barents Shelf (e.g. Rowley & Lottes 1988; Kuzmichev & Pease 2007) (Fig. 2). The three southern islands of the New Siberian Island archipelago are underlain mostly by Jurassic-Cretaceous syn-orogenic sandstones and shales that were shed across the southern margin of the New Siberian platform when it was overridden by allochthonous arc and oceanic rocks of the Anyui Zone (Fig. 2) (Kuzmichev et al. 2005, 2006; Kuzmichev 2009). The syn-orogenic sandstones thus constitute the deposits of a foreland basin that lay to the north and east of the zone of thrust-related deformation. The syn-orogenic foreland basin deposits can be classified into a lower and an upper part representing the initial and the main stages of basin formation.

The first stage of deposition is represented by syn-orogenic deposits in southeastern Big Lyakhov Island where they are partly tectonically buried under the allochthonous ophiolitic assemblage (Kuzmichev et al. 2005; Kuzmichev 2009). They differ from the later-stage deposits by their sandstone composition and more extensive involvement in deformation. The age of these deposits is not reliably confirmed by fossils. They are thought to be Late Jurassic because they contain ophiolitic debris and the ophiolites have been dated as Jurassic (most likely Oxfordian-Kimmeridgian) (Kuzmichev & Lebedev 2008). Triassic-age sandstones and shales are also known to be present in this more highly deformed region (Kuzmichev et al. 2006).

Clastic successions representing the main stage of basin formation crop out in western and northern Big Lyakhov Island and underlie most of Small Lyakhov Island and the Stolbovoi Island (Fig. 2). In the first location they are contact metamorphosed by nearby plutons and were referred to as Volgian only by analogy with similar fossiliferous deposits on Stolbovoi and Small Lyakhov islands (Samusin & Belousova, 1985). On Small Lyakhov Island, Mesozoic sediments are locally exposed at the northern and eastern edges of the Island and were penetrated in several drill-holes in the central part of the Island. On the northeastern shore of the Island, they contain *Buchia* of Volgian-Valanginian age. The same deposits are best exposed on Stolbovoi Island, which is almost completely surrounded by sea cliff exposures.

Stolbovoi Island was visited twice by one of us (Kuzmichev). In 2002, sea cliff exposures on the northwest coast of the island were studied, and the sample discussed in this paper, collected. In 2007, the southern half of the island was investigated in detail and these results are summarized below.

A sand-rich distal turbidite complex underlies Stolbovoi Island. The rocks are slightly altered but preserve all their original sedimentary features. The strata are gently folded and cut by faults. A notable feature of the turbidite complex is the presence of light-colored, medium-grained, amalgamated sandstone units up to 25 meters thick. The detrital zircon sample, discussed below, was obtained from one of these thick sandstone beds. The rest of the complex consists mostly of mud-rich rhythmically bedded, dark-colored sandstones which contain rip-up clasts and plant debris. Shale-silt dominated intervals with minor sandstones with abundant ripples represent a lesser part of the sequence. The massive sand units are interpreted as redeposited in deep water after accumulation on an outer shelf environment. The dark sandstones and shales are interpreted as sediments directly transported from land across a narrow shelf into deep water in the manner described by Mutti et al. (2003). The third facies represents the final deposition of sediments from suspension after the main turbidity current waned.

Sole marks such as tool marks, groove casts and flute casts indicate that sediments were transported from south to north (the mean of 78 measurements is 357°). Ripple marks indicate current directions from the southwest towards the northeast (the mean of 427 measurements is 56.5°). *Buchia* fossils were found in more than 20 locations in the studied area. They were identified by V. A. Zakharov and in general indicate a Late Volgian (Tithonian) to Early Valanginian age.

### Chukotka

Jurassic-Cretaceous strata in exposures north of Bilibino to Pevek on the coast (Fig. 3) were referred to as the Raucha sedimentary basin by Nockleberg (1994, 1998) after Paraketsov & Paraketsov (1989), and as the Myrgovaam Basin by Baranov (1996). Sandstones from the South Anyui Zone have been described in detail by Bondarenko et al. (2003) so our description below focuses on the nature of exposures north of Bilibino.

Most of these sediments are massive, well-cemented, resistant arkosic sandstones that represent gravity flow deposits (probably grain flow and/or amalgamated Bouma A horizons) and contain Volgian (Tithonian) to Valanginian fossils at scattered localities (Akimenko 2000; Belik & Sosunov 1969; Sosunov & Tiliman 1960). Sequences exposed along the coast near Pevek are thinner-bedded gravity flow deposits with lower sand: shale ratios.

The Jurassic-Cretaceous sediments of the Myrgovaam Basin are often described as unconformable on older rocks on map legends and cross-sections. Nockleberg et al. (1994, 1998) classified the sediments as “post-tectonic”. Baranov (1996), however, describes them as structurally detached and imbricated by N-verging thrust sheets. Our field studies (2003, 2004) support Baranov’s conclusions: underlying, Upper Triassic to Lower Jurassic thin bedded shales and sandstones are tightly folded while overlying, massively bedded Jurassic-Cretaceous sandstones form large, coherent fault-imbricated panels. Conglomerates are not found along basal contacts of the overlying massively bedded deposits, but fault zone gouge and breccia are common, suggesting slip along a fault contact. Overlying beds often dip gently into and are truncated by the basal contact, also supporting structural discordance rather than an unconformity (Baranov 1996; Miller et al. 2006). Within

strata mapped as Jurassic-Cretaceous near the Rauchua River, we observed thin-bedded arkosic sandstones in conformable stratigraphic sequence with underlying Jurassic shales. Map-scale conglomeratic lenses, inferred to be submarine channel deposits, cut into these thin-bedded strata and all strata are deformed together in N-vergent open to tight folds (Miller et al. 2006). These relations suggest original stratigraphic continuity between underlying thinner-bedded sequences and overlying massive sandstones. Near Pevek, Jurassic-Cretaceous strata are involved in folds with a south-dipping axial planar cleavage (Miller & Verzhbitsky in press), and thus are clearly involved in at least the latest part of the shortening history of Chukotka.

Poor sorting and angular grains together with fresh plagioclase, K-feldspar, biotite and muscovite point to proximal orogenic sources that contained granitoid/gneissic rocks in addition to sedimentary, metasedimentary and volcanic rocks that are present as abundant lithic fragments in these rocks (Table 1) (Fig. 4). Volcanic lithic fragments are dominated by variable amounts of intermediate to felsic volcanic rocks and rarer mafic volcanic rocks (Fig. 4) (Table 1). Sedimentary and low-grade metasedimentary rocks also form an important component of the sandstones (Table 1). These are mostly fragments of shale, siltstone and multiply deformed slate and phyllite (Fig. 4). Heavy minerals include variable percentages of zircon, apatite, and pyrite, magnetite and ilmenite.

### Detrital zircon data

Detrital zircons from six samples were dated by LA-ICPMS (approximately 100 single grain ages per sample). Sample locations are listed in Table 2, description of analytical methods in Appendix 1, and measured isotopic ratios and interpreted ages in Table 3. The U-Pb ages from each sample are plotted on relative age probability distribution diagrams [Ludwig, 2003] (inset, Fig. 5) and in Figure 6. The Kolmogorov-Smirnov (KS) statistical test was used to further assess the similarity of the distributions of single grain ages and these results are presented in Table 4.

Cumulative age-probability plots (Gehrels 2006), provide the best comparison between data from individual

**Table 2. Locations of samples analyzed for detrital zircon**

Field Number	Area	Lat	Long	Age	Map Unit
GB9986	South Annui Zone	67°17'20"	164°47'13"	J3-K1	(Bondarenko et al., 2003)
CH04 ELM7	Chukotka	68°29'29"	165°41'27.2"	J3-K1	Pogynden Fm.
04JT54C	Chukotka	68°25'19"	166°40'14"	J3-K1	Pogynden Fm.
ELM CH03.24.3	Chukotka	69°09'45.6"	165°02'57.7"	J3-K1	Pogynden Fm.
ELM06 PV10	Pevek, Chukotka	69°43'34.4"	170°57'8.1"	J3-K1	Rauchua Basin, Chauna Fm.
53-1-02	Stolbovoi Is.	74°11'45.3"	135°27'44.9"	J3-K1	Stolbovskaya Fm.

Table III. U-Pb (zircon) geochronologic analyses by Laser-Ablation Multicollector ICP Mass Spectrometry

Analysis	U (ppm)	206Pb			207Pb*			Isotopic ratios			Apparent ages (Ma)			Age of youngest cluster (Ma) (3+ analyses)	
		204Pb			235U			238U (%) corr.			206Pb* ±				
		206Pb*			235U (%)			238U (%) corr.			207Pb* ±				
<b>Sample GB9986 South Annyui Zone</b>															
GB9986-47	136	2214	1,7	0.1467	8	0.02282	1,9	0.24	145.5	2,7	139.0	10,3	29.5	185.3	145.5
GB9986-42	182	862	1,1	0.18368	18,8	0.0234	2,8	0,15	149,1	4,1	171,2	29,7	489,1	414,1	149,1
GB9986-8	152	541	0,6	0.023799	40,9	0.02453	5,3	0,13	156,2	8,2	216,8	79,9	939,1	865,7	156,2
GB9986-24	116	1642	1,6	0.16528	15,8	0.02562	1,8	0,11	163,1	2,9	155,3	22,8	38,7	377,5	163,1
GB9986-103	27	614	1	0.1684	12,7	0.02588	2,5	0,2	164,7	4,1	158,0	18,6	594	297,7	164,7
GB9986-73	107	1639	0,9	0.16719	15,8	0.0261	2,3	0,14	166,1	3,7	157,0	23,0	21,2	377,1	166,1
GB9986-6	586	11572	1,9	0.18473	1,7	0.02726	1	0,59	173,3	1,7	172,1	2,7	155,3	32,0	173,3
GB9986-106	144	3820	0,9	0.1764	7,1	0.02728	1,5	0,21	175,4	2,5	165,0	10,8	17,9	166,3	175,4
GB9986-75	212	4411	1,9	0.18236	4,8	0.02766	3	0,63	175,9	5,2	170,1	7,5	90,2	88,9	175,9
GB9986-53	356	1371	1,6	0.227234	19,7	0.02945	2,8	0,14	187,1	5,2	244,6	42,8	839,9	409,4	187,1
GB9986-64	60	1524	1,3	0.22704	20,2	0.03533	4,4	0,22	223,8	9,7	207,8	37,9	29,0	476,1	223,8
GB9986-56	139	4057	0,9	0.22281	12,1	0.03662	3,4	0,28	231,9	7,8	212,5	23,2	3,1	280,5	231,9
GB9986-25	39	1110	1	0.23828	18,5	0.03748	3,1	0,17	237,2	7,3	217,0	36,2	3,0	442,6	237,2
GB9986-88	568	15023	1,4	0.27206	1,4	0.03842	1	0,7	243,0	2,4	244,3	3,1	257,2	23,6	243,0
GB9986-102	48	1739	0,6	0.25749	17,4	0.04041	1,8	0,11	253,5	4,5	232,6	36,1	27,0	416,5	253,5
GB9986-92	71	1882	2,1	0.25582	13,7	0.04048	2,3	0,17	253,9	5,7	231,3	28,4	7,1	326,9	253,9
GB9986-105	152	5467	1,2	0.21841	4,1	0,0408	1	0,25	257,8	2,5	249,4	9,0	171,2	92,1	257,8
GB9986-62	57	1761	0,5	0.207076	15,5	0.0422	1,4	0,09	266,5	3,7	243,3	33,4	371,0	266,5	37,7
GB9986-23	1228	33907	20,6	0.30144	1,4	0.04261	1	0,71	269,0	2,6	267,5	3,3	254,8	23,1	269,0
GB9986-18	635	9582	2,4	0.31627	2,5	0.04294	1,9	0,74	271,0	5,0	279,0	6,2	346,5	384	271,0
GB9986-81	178	4854	1,3	0.30066	3,9	0.04368	1	0,26	275,6	2,7	266,9	9,2	191,2	88,1	275,6
GB9986-44	103	3297	0,9	0.31956	6	0.04886	1,9	0,32	295,2	5,5	281,6	14,8	169,5	133,4	295,2
GB9986-95	116	3447	0,9	0.3199	5,8	0.04687	1,1	0,19	295,3	3,2	281,8	14,2	171,4	132,4	295,3
GB9986-99	190	6659	1,4	0.33229	3,6	0.04762	1,1	0,31	299,9	3,3	291,8	9,2	227,4	79,3	299,9
GB9986-108	242	9580	3,3	0.34413	1,9	0.04777	1	0,52	300,8	2,9	300,3	5,0	296,4	380	300,8
GB9986-86	195	6316	0,6	0.38456	4	0.05335	1	0,26	341,2	3,5	330,4	11,2	255,1	87,8	341,2
GB9986-27	59	2348	2,1	0.40022	6,6	0.05737	1,9	0,29	359,6	6,7	341,8	19,1	222,5	145,9	359,6
GB9986-59	148	8936	12,8	0.61358	2,7	0.07988	1	0,37	495,4	4,8	485,8	10,4	440,8	55,9	495,4
GB9986-38	59	3869	0,7	0.88098	6,4	0.10918	2,7	0,42	668,0	16,9	641,5	30,4	549,3	126,7	668,0
GB9986-57	102	10912	1,1	1.35739	1,8	0.14374	1,4	0,82	865,8	11,7	870,7	10,3	883,4	21,1	865,8
GB9986-110	212	38602	2,8	1.73346	1,5	0.17205	1	0,68	1023,4	9,5	1021,0	9,5	1016,0	21,9	1016,0
GB9986-58	152	33922	1,8	5.24523	1,4	0.33377	1	0,71	1856,6	16,1	1860,0	12,1	1863,8	18,1	1863,8
GB9986-17	376	51988	2,9	4.07792	1,5	0.25914	1,1	0,73	1485,4	14,3	1649,9	12,0	1866,2	18,1	1866,2
GB9986-10	90	19309	2	4.72569	1,6	0.30021	1,2	0,78	1692,3	18,5	1771,8	13,4	1866,8	18,1	1866,8
GB9986-22	179	38171	54	4.97025	1,8	0.31561	1,1	0,62	1768,2	17,4	1814,3	15,5	1867,5	26,0	1867,5
GB9986-109	337	102143	2,3	5.25163	1,7	0.33267	1	0,58	1851,3	16,1	1861,0	14,7	1871,9	25,3	1871,9
GB9986-14	47	9779	1,4	5.57433	5	0.35178	4,9	0,98	1943,1	82,4	1912,1	43,2	1878,7	18,2	1878,7
GB9986-79	397	68076	2,3	4.48327	1,4	0.28998	1	0,71	1596,3	14,1	1727,9	11,7	1891,2	18,0	1891,2
GB9986-61	216	46985	2	5.30987	1,4	0.33274	1	0,71	1851,7	16,1	1870,5	12,1	1891,4	18,0	1891,4
GB9986-83	314	27072	4,1	4.69086	4,9	0.29393	4,6	0,94	1661,2	68,1	1765,6	41,4	1891,5	30,1	1891,5
GB9986-26	186	37074	2,2	5.535567	1,4	0.33514	1	0,71	1863,2	16,2	1877,8	12,1	1893,9	18,0	1893,9
GB9986-3	38	10529	0,9	5.51568	1,6	0.34389	1	0,64	1905,3	16,5	1907,0	13,4	1900,5	21,5	1900,5
GB9986-12	270	54750	1,3	5.56777	1,5	0.34654	1,1	0,75	1918,1	19,1	1911,1	13,1	1903,6	18,0	1903,6
GB9986-84	33	5322	1,2	5.16903	3,1	0.32101	2,9	0,94	1794,7	45,6	1847,5	26,2	1907,6	18,1	1907,6

145 (3)

164 (3)

Analysis	U (ppm)	206Pb	207Pb*	U/Th	235U	238U	206Pb*	238U (%)	corr.	error	206Pb*	235U (Ma)	207Pb* (Ma)	207Pb* ± (Ma)	206Pb* ± (Ma)	Best age (Ma)	± (Ma)	Apparent ages (Ma)	
																		Age of youngest cluster (Ma) (3+ analyses)	
GB9986-29	315	71378	1.6	5,61742	1.5	0.34846	1	0.66	1927.2	16.7	1918.8	13.1	1909.6	20.6	1909.6	20.6	1909.6	20.6	
GB9986-72	666	119208	30.2	4,80903	1.6	0.29773	1.1	0.68	1680.0	16.1	1786.5	13.5	1913.2	21.0	1913.2	21.0	1913.2	21.0	
GB9986-63	370	73771	2	5,20857	2.8	0.32329	2.7	0.94	1801.4	41.7	1854.0	24.2	1913.6	17.9	1913.6	17.9	1913.6	17.9	
GB9986-65	231	52468	3	5,64787	1.4	0.34923	1	0.71	1930.9	16.7	1923.4	12.2	1915.4	17.9	1915.4	17.9	1915.4	17.9	
GB9986-76	179	38446	0.9	5,54102	1.8	0.34249	1.4	0.79	1898.6	23.2	1907.0	15.4	1916.1	19.9	1916.1	19.9	1916.1	19.9	
GB9986-98	529	110343	7.1	5,82758	1.8	0.35914	1	0.55	1978.1	17.0	1950.5	15.6	1921.4	26.9	1921.4	26.9	1921.4	26.9	
GB9986-91	81	21704	1.5	5,72859	1.6	0.35294	1	0.62	1948.6	16.8	1935.7	14.0	1921.9	22.8	1921.9	22.8	1921.9	22.8	
GB9986-7	165	42095	2.2	5,73997	3.5	0.35345	3.2	0.93	1951.0	54.2	1937.4	30.0	1922.8	22.8	1922.8	22.8	1922.8	22.8	
GB9986-20	78	18418	2.4	5,63824	1.5	0.34699	1	0.67	1920.2	16.7	1922.0	12.9	1923.9	19.9	1923.9	19.9	1923.9	19.9	
GB9986-77	420	91758	3.5	5,74615	1.5	0.35325	1	0.66	1950.1	16.8	1938.3	13.1	1925.8	20.3	1925.8	20.3	1925.8	20.3	
GB9986-107	105	34289	0.7	5,68546	1.4	0.34949	1	0.71	1932.1	16.7	1929.2	12.2	1925.9	17.9	1925.9	17.9	1925.9	17.9	
GB9986-33	1274	207975	50.4	5,7373	1.4	0.35255	1	0.71	1946.8	16.8	1937.0	12.2	1926.5	17.9	1926.5	17.9	1926.5	17.9	
GB9986-13	154	22854	2.9	5,90727	1.6	0.36296	1.2	0.75	1996.2	20.6	1962.3	13.9	1926.7	18.8	1926.7	18.8	1926.7	18.8	
GB9986-67	301	27369	1.9	5,5979	1.5	0.34396	1.1	0.73	1905.7	17.5	1915.8	12.6	1926.7	18.0	1926.7	18.0	1926.7	18.0	
GB9986-37	81	22806	9.4	5,74755	1.6	0.35173	1	0.64	1942.9	16.8	1938.5	13.5	1933.9	21.4	1933.9	21.4	1933.9	21.4	
GB9986-82	195	40128	4.2	5,6174	1.4	0.34322	1	0.71	1902.1	16.5	1918.8	12.2	1936.8	17.9	1936.8	17.9	1936.8	17.9	
GB9986-96	630	119224	2.8	5,86726	1.8	0.35844	1	0.59	1974.8	17.5	1956.4	15.2	1937.0	25.4	1937.0	25.4	1937.0	25.4	
GB9986-94	211	40463	1.3	5,39123	2.1	0.32919	1.6	0.8	1834.4	26.2	1883.5	17.6	1938.0	22.2	1938.0	22.2	1938.0	22.2	
GB9986-78	757	155999	29.8	5,64736	2.8	0.34479	1.1	0.4	1909.7	18.8	1923.4	24.2	1938.1	46.0	1938.1	46.0	1938.1	46.0	
GB9986-60	374	68792	9.9	5,98706	1.5	0.36508	1	0.67	2006.2	17.2	1974.0	12.9	1940.3	19.7	1940.3	19.7	1940.3	19.7	
GB9986-71	35	10094	8.5	5,86619	2.8	0.35761	2.4	0.87	1970.8	40.5	1956.2	23.9	1940.8	24.6	1940.8	24.6	1940.8	24.6	
GB9986-28	601	129251	6	5,81539	1.5	0.35547	1	0.69	1951.2	16.8	1948.7	12.6	1946.1	18.8	1946.1	18.8	1946.1	18.8	
GB9986-74	187	39603	5.3	5,77696	2.4	0.35091	1.9	0.79	1938.9	31.9	1943.0	20.8	1947.3	26.3	1947.3	26.3	1947.3	26.3	
GB9986-50	650	129605	5.7	5,87798	1.4	0.35663	1	0.71	1966.2	16.9	1958.0	12.3	1949.3	17.9	1949.3	17.9	1949.3	17.9	
GB9986-49	582	74160	3.5	5,89296	1.4	0.35104	1	0.71	1939.5	16.7	1946.9	12.3	1954.6	17.9	1954.6	17.9	1954.6	17.9	
GB9986-70	492	94094	2.3	5,75824	1.6	0.3482	1.2	0.73	1926.0	19.3	1940.2	13.8	1955.3	19.5	1955.3	19.5	1955.3	19.5	
GB9986-97	390	50803	6.4	5,79483	1.4	0.34948	1	0.71	1932.1	16.7	1945.6	12.2	1960.0	17.8	1960.0	17.8	1960.0	17.8	
GB9986-101	169	53259	2.9	6,08352	1.9	0.3645	1.1	0.57	2003.5	19.0	1987.9	16.9	1971.7	28.5	1971.7	28.5	1971.7	28.5	
GB9986-2	1081	19948	6.4	5,91898	1.4	0.35394	1	0.71	1953.4	16.9	1964.0	12.3	1975.2	17.8	1975.2	17.8	1975.2	17.8	
GB9986-43	320	59899	1.3	5,83416	1.5	0.34867	1	0.68	1928.2	16.7	1951.5	12.8	1976.2	19.4	1976.2	19.4	1976.2	19.4	
GB9986-34	432	99478	12.2	5,94355	2.1	0.35356	1.2	0.59	1951.6	20.6	1967.6	18.1	1984.5	30.1	1984.5	30.1	1984.5	30.1	
GB9986-80	365	93207	1.4	6,2029	2	0.36409	1	0.52	2001.5	17.8	2004.9	17.5	2008.3	30.5	2008.3	30.5	2008.3	30.5	
GB9986-36	82	5196	2.4	5,99187	5.5	0.35697	4.9	0.9	1939.2	82.5	1974.7	47.6	2012.0	42.1	2012.0	42.1	2012.0	42.1	
GB9986-54	263	14810	3	5,94157	1.6	0.35239	1	0.63	1946.0	16.8	1967.3	13.9	1989.8	22.2	1989.8	22.2	1989.8	22.2	
GB9986-16	757	103016	1.8	6,11608	1.6	0.36253	1.2	0.76	1994.1	20.8	1992.5	13.9	1990.9	18.5	1990.9	18.5	1990.9	18.5	
GB9986-9	414	78599	5	6,27499	2.4	0.37074	2	0.82	2032.9	34.3	2015.0	21.0	1996.7	24.3	1996.7	24.3	1996.7	24.3	
GB9986-85	210	49345	3.3	6,1651	1.4	0.35818	1	0.71	1973.6	17.0	1999.5	12.4	2026.4	17.7	2026.4	17.7	2026.4	17.7	
GB9986-30	262	37870	2.6	6,44545	1.8	0.37048	1	0.58	2031.6	18.1	2038.5	15.8	2045.4	25.8	2045.4	25.8	2045.4	25.8	
GB9986-5	478	7816	2.6	6,28763	1.8	0.35243	1.2	0.68	1946.2	20.9	2016.7	16.1	2089.7	23.8	2089.7	23.8	2089.7	23.8	
GB9986-32	782	192851	6.1	9,05007	1.9	0.40702	1	0.52	2201.3	18.7	2343.1	17.6	2469.0	27.7	2469.0	27.7	2469.0	27.7	
GB9986-48	144	48029	1.9	10,78956	2	0.48066	1.4	0.68	2530.2	29.1	2505.2	18.9	2485.0	25.0	2485.0	25.0	2485.0	25.0	
GB9986-93	558	105849	2.6	10,97883	1.5	0.47958	1	0.69	2552.5	13.6	2518.0	17.8	2518.0	17.8	2518.0	17.8	2518.0	17.8	
GB9986-69	204	56363	2.3	10,26958	2	0.4465	1.5	0.73	2379.7	29.4	2459.4	18.7	2525.9	23.2	2525.9	23.2	2525.9	23.2	
GB9986-21	172	23121	5.1	10,1396	6.1	0.43018	5.5	0.9	2306.5	106.3	2447.6	56.1	2566.9	43.3	2566.9	43.3	2566.9	43.3	
GB9986-31	73	25538	1.3	11,34675	2	0.47466	1.4	0.72	2511.8	30.1	2552.1	18.8	2584.2	23.4	2584.2	23.4	2584.2	23.4	
GB9986-4	570	162075	6	12,07632	1.9	0.50358	1.6	0.84	2629.1	35.1	2610.3	18.2	2595.8	17.7	2595.8	17.7	2595.8	17.7	

Analysis	U (ppm)	206Pb	207Pb*	U/Th	207Pb*	Isotopic ratios				Apparent ages (Ma)				Age of youngest cluster (Ma) (3+ analyses)		
						235U (%)	238U (%)	206Pb* ± error	238U (Ma)	235U (Ma)	207Pb* ± error	207Pb* (Ma)	206Pb* (Ma)	Best age (Ma)	± (Ma)	
GB9986-11	335	97124	2,7	11.83485	1,6	0.48785	1	0.63	2561.4	21,1	2591.4	14.8	2615.0	20.5	2615.0	20.5
GB9986-35	246	85572	4,6	12.09953	3,5	0.49438	1,6	0.46	2589.6	34,9	2612,2	33,2	2629,7	52,2	2629,7	52,2
GB9986-19	325	83725	2,1	11.84248	1,5	0.47987	1	0.68	2552,7	20,9	2592,0	13,7	2643,5	17,8	2643,5	17,8
GB9986-51	104	34709	1,6	12.61437	1,7	0.50953	1,4	0.81	2654,6	29,8	2651,3	16,0	2648,7	16,6	2648,7	16,6
GB9986-52	52	12645	1,6	13.00456	2,2	0.51909	1,7	0.77	2695,3	37,7	2680,0	21,0	2668,4	23,7	2668,4	23,7
GB9986-104	298	110030	1,2	12.94821	2,1	0.51524	1,9	0.88	2679,4	40,6	2675,9	19,8	2673,0	16,6	2673,0	16,6
GB9986-40	90	29013	0,9	13.15951	1,8	0.52057	1,3	0.76	2701,6	29,8	2691,2	16,7	2683,3	19,0	2683,3	19,0
GB9986-15	298	91953	1,5	12.94075	1,4	0.50805	1	0.71	2648,3	21,7	2675,3	13,3	2695,8	16,5	2695,8	16,5
GB9986-66	129	50276	1,4	14.17815	3,5	0.54291	3,4	0.96	2795,6	76,6	2761,7	33,4	2737,0	16,5	2737,0	16,5
GB9986-68	116	42597	1,6	13.74526	1,4	0.52342	1	0.71	2713,7	22,1	2732,3	13,4	2746,1	16,4	2746,1	16,4
GB9986-45	317	93698	3,6	19.30147	1,4	0.592	1	0.71	2997,5	24,0	3057,0	13,7	3096,3	15,9	3096,3	15,9
<b>Sample CH04ELM7 Chukotka</b>														157 (6)		
CH04ELM7-40	192	4702	1	0.15919	7,8	0.02465	1,9	0.25	156,9	3,0	150,0	10,9	41,4	181,3	156,9	3,0
CH04ELM7-40	58	943	1,4	0.15966	40,6	0.02492	4	0,1	158,7	6,3	150,4	56,8	21,9	1006,2	158,7	6,3
CH04ELM7-61	38	960	1,3	0.16265	53,6	0.02527	9,3	0,17	160,8	14,7	153,0	76,3	33,4	1354,1	160,8	14,7
CH04ELM7-55	30	555	1,4	0.16241	55,5	0.02539	5,3	0,1	161,6	8,5	152,8	78,9	18,4	143,4	161,6	8,5
CH04ELM7-49	66	1529	1,2	0.16358	49	0.02567	4,3	0,09	163,4	6,9	153,8	70,1	8,8	1243,3	163,4	6,9
CH04ELM7-26	62	2360	1,7	0.17123	15,8	0.02679	3	0,19	170,5	5,1	160,5	23,5	15,8	374,6	170,5	5,1
CH04ELM7-12	56	1738	2,6	0.17174	20,9	0.02702	4,3	0,2	171,9	7,3	160,9	31,2	2,7	497,8	171,9	7,3
CH04ELM7-35	79	2357	1,4	0.23515	11,7	0.03685	2,1	0,18	233,3	4,8	214,4	22,6	11,9	277,3	233,3	4,8
CH04ELM7-48	172	5570	2,9	0.24829	8,3	0.03821	1,6	0,19	241,8	3,8	245,2	16,8	55,5	195,3	241,8	3,8
CH04ELM7-59	137	4017	2,8	0.25492	7,3	0.03874	2,6	0,35	245,0	6,3	230,6	15,1	85,6	162,7	245,0	6,3
CH04ELM7-44	77	2417	1,2	0.25209	13,3	0.03892	2,9	0,22	246,1	6,9	228,3	27,2	48,2	311,4	246,1	6,9
CH04ELM7-109	85	3580	0,7	0.25255	11,5	0.03924	1,8	0,15	248,1	4,3	228,6	23,6	32,7	274,1	248,1	4,3
CH04ELM7-20	126	4721	2,2	0.25473	9,3	0.03936	1,9	0,2	248,8	4,6	230,4	19,2	46,3	218,0	248,8	4,6
CH04ELM7-96	75	3003	1,2	0.2599	27,4	0.04009	3,5	0,13	253,4	8,8	234,6	57,5	50,0	659,7	253,4	8,8
CH04ELM7-84	234	2163	2,6	0.32104	5,1	0.04064	2,2	0,43	256,8	5,5	282,7	12,6	50,3	101,5	256,8	5,5
CH04ELM7-16	331	8892	1,2	0.28342	2,5	0.04065	1,6	0,66	256,9	4,1	253,4	5,5	220,9	43,1	256,9	4,1
CH04ELM7-36	176	8609	0,5	0.28822	2,9	0,04151	1,2	0,41	262,2	3,0	257,2	6,5	21,1,5	60,7	262,2	3,0
CH04ELM7-9	574	1515	2,3	0.37761	8,6	0.04228	5,9	0,69	267,0	15,4	322,3	23,8	767,0	131,4	267,0	15,4
CH04ELM7-83	142	3872	1	0.28542	6	0.0424	2,1	0,34	267,7	5,4	255,0	13,5	139,1	132,1	267,7	5,4
CH04ELM7-71	43	3179	1	0.33918	14,4	0.05233	3,4	0,24	328,8	10,9	296,5	37,0	49,7	335,3	328,8	10,9
CH04ELM7-62	113	3080	1,2	0.41497	3,7	0.05399	1,8	0,5	339,0	6,0	352,4	10,9	44,2,3	70,6	339,0	6,0
CH04ELM7-73	68	3671	0,8	0.37315	10,3	0.0589	1,2	0,11	350,6	4,0	322,0	28,5	119,8	242,5	350,6	4,0
CH04ELM7-81	41	2223	0,6	0.44758	10,6	0.0583	3,4	0,32	365,3	11,9	375,6	33,2	439,8	223,2	365,3	11,9
CH04ELM7-86	51	2904	1,1	0.40424	9,3	0.05915	2,7	0,29	370,4	9,7	344,7	27,2	407,6	370,4	9,7	370,4
CH04ELM7-67	62	5880	1,9	0.54084	6,6	0.07417	2,1	0,31	445,0	9,0	439,0	23,6	407,6	140,9	445,0	9,0
CH04ELM7-38	30	9040	1,3	4.53723	2,4	0.30977	1,1	0,48	1739,6	17,2	1737,8	19,6	1735,7	38,0	1735,7	38,0
CH04ELM7-92	31	9573	1,7	4.56824	2,1	0.31043	1,7	0,81	1742,8	26,5	1739,8	17,7	1736,2	22,6	1736,2	22,6
CH04ELM7-98	47	12385	2,4	4.55706	1,7	0.30885	1,1	0,69	1735,1	17,4	1741,5	13,9	1749,1	22,1	1749,1	22,1
CH04ELM7-94	858	56032	19,7	4.19924	2,3	0.27153	2,1	0,89	1548,6	28,6	1673,9	19,2	1834,7	19,6	1834,7	19,6
CH04ELM7-31	144	32453	0,8	5.32685	3,3	0.34003	2,7	0,82	1886,8	44,7	1873,2	28,6	1858,1	34,7	1858,1	34,7
CH04ELM7-33	224	66914	5,8	5,10123	2,7	0.32096	2,4	0,88	1794,4	37,9	1836,3	23,3	1884,1	23,4	1884,1	23,4
CH04ELM7-1	24	8139	3,4	4.78307	3,1	0.30022	2,5	0,81	1692,4	37,7	1781,9	26,2	1884,4	32,8	1884,4	32,8
CH04ELM7-65	115	36174	1,6	5.58793	1,9	0.34949	1,6	0,85	1932,2	27,5	1914,2	16,6	1894,9	18,0	1894,9	18,0
CH04ELM7-69	62	20112	0,7	5.56116	1,8	0.34717	1,3	0,72	1921,1	22,1	1910,1	15,8	1898,2	22,7	1898,2	22,7
CH04ELM7-85	99	42128	4,5	5.55592	1,6	0.34519	1	0,63	1911,6	16,5	1909,3	13,6	1906,8	21,9	1906,8	21,9
CH04ELM7-78	51	16952	1,7	5.5997	1,7	0,34749	1,4	0,8	1924,5	22,6	1916,1	14,6	1906,9	18,1	1906,9	18,1

Analysis	U (ppm)	204Pb	206Pb	U/Th	207Pb*	Isotopic ratios			Apparent ages (Ma)					Age of youngest cluster (Ma) (3+ analyses)				
						235U	238U	(%)	206Pb*	±	206Pb*	±	207Pb*	±	207Pb*	±	Best age	±
CH04ELM7-91	51	20781	1.5	5,60795	1.8	0.34777	1.4	0.8	1923.9	23.8	1917.3	15.3	1910.2	18.9	1910.2	18.9		
CH04ELM7-34	159	60323	2	5,7031	1.6	0.35364	1.2	0.77	1951.9	20.1	1931.8	13.5	1910.3	18.0	1910.3	18.0		
CH04ELM7-52	181	55857	1.8	5,61568	2.4	0.34809	1.1	0.46	1925.5	18.6	1918.5	21.1	1911.0	39.1	1911.0	39.1		
CH04ELM7-7	141	38242	1.1	5,33697	4.5	0.33194	4.1	0.9	1847.8	65.3	1878.0	38.6	1911.6	35.2	1911.6	35.2		
CH04ELM7-28	87	29963	2.5	5,45406	1.7	0.33759	1	0.57	1875.0	16.3	1893.4	15.0	1913.6	25.7	1913.6	25.7		
CH04ELM7-80	294	79596	3.2	5,73323	1.9	0.35452	1.4	0.77	1956.2	24.2	1936.4	16.2	1915.3	21.5	1915.3	21.5		
CH04ELM7-93	34	12670	5.4	5,49239	1.7	0.33961	1.1	0.66	1884.8	18.1	1899.4	14.4	1915.4	22.6	1915.4	22.6		
CH04ELM7-100	155	58246	1.3	5,62561	2.2	0.34759	1	0.46	1923.1	16.6	1920.0	18.8	1916.7	34.8	1916.7	34.8		
CH04ELM7-110	99	43479	1.5	5,62715	2.3	0.348	1.4	0.61	1925.0	23.1	1921.8	19.7	1918.3	32.5	1918.3	32.5		
CH04ELM7-64	129	31543	1.7	5,62325	2	0.34764	1.6	0.81	1923.3	26.5	1921.1	17.0	1918.6	20.7	1918.6	20.7		
CH04ELM7-24	286	78465	1.4	5,43746	1.4	0.3335	1	0.71	1865.0	16.2	1890.8	12.1	1919.2	17.9	1919.2	17.9		
CH04ELM7-107	86	33424	0.9	5,54845	1.9	0.34201	1.4	0.71	1896.3	22.5	1908.1	16.6	1921.0	24.4	1921.0	24.4		
CH04ELM7-17	165	34727	0.5	5,61864	1.6	0.34562	1	0.61	1913.7	16.6	1919.0	14.2	1924.7	23.5	1924.7	23.5		
CH04ELM7-87	693	161668	8.3	5,64937	1.8	0.34746	1.5	0.84	1922.5	25.4	1923.7	15.8	1924.9	17.9	1924.9	17.9		
CH04ELM7-46	95	32329	0.6	5,66337	1.8	0.34791	1.5	0.83	1924.6	24.9	1925.9	15.6	1927.2	18.0	1927.2	18.0		
CH04ELM7-30	104	36892	0.6	5,55654	1.5	0.34105	1	0.65	1891.7	16.4	1909.4	13.3	1928.6	21.2	1928.6	21.2		
CH04ELM7-70	510	114482	4.9	5,68546	2.6	0.34888	2.1	0.83	1929.7	35.3	1929.2	22.0	1928.6	25.4	1928.6	25.4		
CH04ELM7-95	266	82289	0.9	5,67826	2.6	0.34846	1.2	0.44	1927.3	19.5	1928.1	22.8	1928.9	42.5	1928.9	42.5		
CH04ELM7-53	408	124343	5.5	5,60409	1.9	0.34334	1.3	0.71	1903.7	21.9	1916.9	16.1	1931.1	23.5	1931.1	23.5		
CH04ELM7-2	146	53762	3.1	5,65166	1.4	0.34591	1	0.71	1915.0	16.6	1924.0	12.2	1933.7	17.9	1933.7	17.9		
CH04ELM7-99	138	35858	1.6	5,65659	2.6	0.34595	1.3	0.51	1915.2	21.9	1924.8	22.5	1935.1	40.1	1935.1	40.1		
CH04ELM7-18	262	63509	4.5	5,62416	2.2	0.34394	1.2	0.56	1905.6	19.8	1919.8	18.7	1935.2	32.2	1935.2	32.2		
CH04ELM7-79	290	119961	7.4	5,7965	2.6	0.35437	1.3	0.5	1955.4	22.0	1945.9	22.8	1935.7	41.0	1935.7	41.0		
CH04ELM7-88	209	64463	0.7	5,75441	1.5	0.35167	1.1	0.73	1942.6	18.0	1939.6	12.7	1936.4	17.9	1936.4	17.9		
CH04ELM7-19	326	75510	2.5	5,70411	1.4	0.34818	1	0.71	1925.9	16.6	1932.0	12.2	1938.5	17.9	1938.5	17.9		
CH04ELM7-6	475	157002	5.1	5,67337	2.5	0.34613	1.9	0.77	1916.1	31.7	1927.3	21.4	1939.4	28.3	1939.4	28.3		
CH04ELM7-74	505	90528	3.8	5,71605	2.3	0.34812	1.4	0.6	1925.6	23.2	1933.8	20.2	1942.6	33.5	1942.6	33.5		
CH04ELM7-14	132	33221	2	5,57591	1.8	0.33933	1.1	0.6	1883.9	17.4	1912.4	15.2	1943.4	25.3	1943.4	25.3		
CH04ELM7-97	825	190476	1.1	5,67028	3.2	0.34504	2	0.62	1910.9	33.0	1926.9	27.7	1944.1	44.9	1944.1	44.9		
CH04ELM7-10	42	83358	2.7	5,493	4.5	0.33333	3.1	0.69	1853.6	49.6	1899.5	38.3	1950.1	57.5	1950.1	57.5		
CH04ELM7-21	662	72255	3	5,7646	2.2	0.3495	1	0.46	1932.2	16.7	1941.1	18.9	1950.6	34.7	1950.6	34.7		
CH04ELM7-58	159	32794	1.2	5,55766	1.8	0.33673	1.2	0.67	1870.9	19.4	1909.6	15.3	1951.8	23.4	1951.8	23.4		
CH04ELM7-108	301	22678	2.8	5,6093	3.2	0.33957	2	0.63	1884.6	33.3	1917.5	27.8	1953.3	44.7	1953.3	44.7		
CH04ELM7-27	78	29817	1.3	5,77452	1.4	0.34925	1	0.72	1931.0	17.2	1942.6	12.5	1955.0	18.0	1955.0	18.0		
CH04ELM7-57	48	14936	2.5	6,06877	2.2	0.36669	1.3	0.61	2013.8	22.6	1985.8	18.8	1956.7	30.7	1956.7	30.7		
CH04ELM7-60	90	31482	2	5,76451	2.9	0.34777	1.3	0.44	1923.9	21.3	1941.1	25.3	1959.5	47.0	1959.5	47.0		
CH04ELM7-25	487	103048	4.3	5,79516	1.4	0.34953	1	0.69	1932.3	16.7	1945.7	12.2	1976.7	17.8	1976.7	17.8		
CH04ELM7-15	168	40481	1.2	5,62719	6.7	0.33927	6.4	0.96	1883.2	104.6	1920.3	57.4	1960.6	32.0	1960.6	32.0		
CH04ELM7-22	6515	1.5	5,85782	2.5	0.35274	2	0.79	1947.7	33.2	1955.0	21.6	1962.8	26.9	1962.8	26.9			
CH04ELM7-51	1611	41637	1.1	5,97779	2.6	0.35957	1.7	0.66	1980.1	28.8	1972.6	22.3	1964.7	34.4	1964.7	34.4		
CH04ELM7-13	101	24917	1.5	5,83569	2.9	0.35052	2.2	0.76	1937.1	37.4	1951.7	25.4	1967.3	33.8	1967.3	33.8		
CH04ELM7-37	239	46781	1.8	5,78789	1.4	0.34582	1	0.71	1914.6	16.6	1944.6	12.2	1976.7	17.8	1976.7	17.8		
CH04ELM7-22	326	58498	4	5,96617	4.2	0.35643	3.6	0.86	1965.2	60.5	1971.1	36.2	1977.2	38.3	1977.2	38.3		
CH04ELM7-50	467	115927	1.8	6,14226	2.6	0.36589	1.1	0.43	2010.0	19.5	1996.3	22.8	1982.1	41.8	1982.1	41.8		
CH04ELM7-42	87	28855	1.8	6,40132	1.6	0.37753	1.2	0.76	2064.7	21.5	2032.4	14.1	1999.8	18.6	1999.8	18.6		
CH04ELM7-25	242	133380	3.4	6,41633	2.1	0.37838	1.5	0.74	2068.7	27.4	2034.5	18.5	2000.0	25.2	2000.0	25.2		
CH04ELM7-23	121	30965	2.7	6,02352	2.1	0.35436	1	0.49	1955.4	17.0	1979.2	18.1	2004.3	32.2	2004.3	32.2		
CH04ELM7-45	73	23167	2	6,30193	1.5	0.37071	1.2	0.76	2032.7	20.5	2018.7	13.5	2004.4	17.8	2004.4	17.8		
CH04ELM7-105	89	37114	2.8	6,10672	1.9	0.35919	1.3	0.66	1978.3	21.4	1991.2	16.5	2004.6	25.2	2004.6	25.2		

Analysis	U (ppm)	206Pb	207Pb*	U/Th	207Pb*	Isotopic ratios				Apparent ages (Ma)				Age of youngest cluster (Ma) (3+ analyses)
						235U (%)	238U (%)	error corr.	206Pb* ±	238U (Ma)	235U (Ma)	207Pb* ±	207Pb* (Ma)	
CH04ELM7-106	79	38884	1.4	6.20238	2.6	0.36472	1.5	0.59	2004.5	26.5	2004.8	22.8	2005.1	37.5
CH04ELM7-68	96	29344	1.3	6.04669	2.4	0.3552	1.9	0.81	1959.4	32.9	1982.6	20.9	2006.9	24.9
CH04ELM7-103	89	37630	1.2	6.33077	2	0.36945	1.7	0.86	2026.8	30.3	2022.7	17.7	2018.5	18.3
CH04ELM7-101	517	163931	1.3	6.15631	3	0.3564	2	0.66	1965.1	33.7	1998.3	26.4	2032.7	40.4
CH04ELM7-72	160	58804	1.5	6.49308	1.6	0.37067	1	0.62	2032.5	17.8	2045.0	14.4	2057.5	22.6
CH04ELM7-66	647	8718	3.7	5.25637	8.6	0.29985	7.4	0.87	1690.6	110.7	1861.8	73.3	2058.8	75.2
CH04ELM7-11	155	41358	2.2	6.45715	3.9	0.36482	3.3	0.86	2005.0	57.4	2040.1	34.0	2075.7	34.4
CH04ELM7-104	338	46084	0.7	6.7529	3.8	0.37079	3.2	0.84	2033.1	55.6	2079.6	33.6	2125.9	35.9
CH04ELM7-90	7611	211176	13.4	6.87514	3.1	0.35752	2.7	0.86	1970.4	46.2	2095.5	27.9	2220.6	27.4
CH04ELM7-3	445	124138	4.5	9.35644	2.9	0.44296	2	0.67	2363.9	38.8	2373.6	26.7	2381.9	36.6
CH04ELM7-39	359	77484	1.8	10.19447	2.6	0.47526	1.5	0.57	2506.6	30.7	2452.6	23.8	2408.1	35.9
CH04ELM7-56	357	94639	1.4	13.04338	2.1	0.50445	1	0.48	2632.9	21.6	2682.8	19.7	2720.6	30.2
CH04ELM7-32	69	39136	1.5	1.05109	1.8	0.50402	1.1	0.62	2631.0	24.6	2683.4	17.2	2730.0	23.6
CH04ELM7-89	68	35838	1.2	13.19657	1.6	0.50727	1.3	0.79	2645.0	27.7	2693.8	15.3	2730.6	16.5
CH04ELM7-29	115	52881	1.8	13.757	1.6	0.52116	1.1	0.71	2706.7	24.8	2733.1	15.0	2752.7	18.4
CH04ELM7-5	146	74941	1.3	14.1134	1.5	0.53483	1	0.67	2761.8	22.5	2757.4	14.2	2754.1	18.2
CH04ELM7-41	482	131361	1.8	14.52673	1.9	0.54387	1.4	0.76	2799.6	32.2	2784.8	17.8	2774.0	20.2
CH04ELM7-77	223	106009	1.1	14.3725	2.6	0.53282	1.9	0.74	2753.3	42.2	2774.6	24.3	2790.1	28.3
<b>Sample 04T54 Chukotka</b>														159 (8); 175 (8)
04T54C-6	57	1521	0.7	0.15564	35	0.02451	5.7	0.16	156.1	8.9	146.9	47.9	0.6	855.4
04T54C-98	157	3062	0.8	0.16148	17.9	0.02491	1.9	0.11	158.6	3.0	152.0	25.2	50.2	427.1
04T54C-45	36	769	0.9	0.16255	47.4	0.02498	7.4	0.16	159.1	11.6	152.9	67.4	58.7	1176.4
04T54C-40	55	1143	1.1	0.16456	26.7	0.0257	5.3	0.2	163.6	8.6	154.7	38.3	20.9	636.7
04T54C-97	47	1206	1.8	0.16997	19.2	0.02619	7.6	0.4	166.7	12.6	159.2	28.3	48.8	423.8
04T54C-13	40	872	1.4	0.17144	54.1	0.0266	5.8	0.11	169.2	9.7	160.7	80.6	36.1	1383.4
04T54C-7	60	1732	1.4	0.17088	14.2	0.02662	5.5	0.39	169.3	9.3	160.2	21.0	26.9	314.8
04T54C-32	111	1976	1.2	0.18476	9.6	0.02724	4.2	0.43	173.3	7.1	172.1	15.2	156.6	202.4
04T54C-101	155	3997	3.3	0.17764	6.3	0.02744	2.8	0.44	174.5	4.8	166.0	9.7	46.6	136.4
04T54C-11	163	4021	1.1	0.17944	8.6	0.02776	1.4	0.17	176.5	2.5	167.6	13.2	43.0	202.1
04T54C-49	90	2910	1.8	0.24328	7	0.03674	2.8	0.39	232.6	6.3	222.1	14.0	100.1	152.9
04T54C-25	101	2676	1.6	0.26602	4.8	0.03833	2.2	0.47	241.8	5.3	239.5	10.2	216.8	97.8
04T54C-105	85	2310	0.8	0.24872	12.7	0.03829	3	0.24	242.2	7.2	225.5	25.7	54.9	295.8
04T54C-5	41	2008	0.5	0.24661	13.1	0.0386	4.6	0.35	244.1	10.9	223.8	26.4	154	297.2
04T54C-102	134	5073	1.8	0.26221	4.4	0.03866	1.7	0.39	244.5	4.2	236.4	9.4	157.1	95.9
04T54C-49	64	1786	0.6	0.25099	17.5	0.03867	2.4	0.14	244.6	5.8	227.4	35.7	52.9	416.5
04T54C-68	218	6665	0.5	0.27753	4.1	0.04069	1.1	0.26	257.1	2.7	248.7	9.1	170.1	93.4
04T54C-44	95	2769	0.9	0.25007	4.1	0.04076	3.4	0.84	257.5	8.7	262.9	9.5	311.1	50.5
04T54C-100	432	7711	1.5	0.27568	2.7	0.03926	1.2	0.45	248.2	2.9	247.2	5.9	237.8	248.2
04T54C-67	210	4209	1.5	0.27947	5.8	0.03975	1.8	0.3	251.3	4.3	250.2	12.9	240.6	128.0
04T54C-10	42	1307	0.7	0.25865	18.7	0.04002	4.4	0.23	253.0	10.9	233.6	39.1	42.5	438.5
04T54C-46	218	8985	0.7	0.29552	4.1	0.04076	3.4	0.84	257.5	8.7	262.9	9.5	311.1	50.5
04T54C-56	597	624	3.3	0.30505	18.9	0.04222	6.1	0.32	266.6	15.9	270.3	45.0	303.0	411.9
04T54C-43	79	1922	0.8	0.3007	12.2	0.0429	3.7	0.3	270.8	9.8	266.9	28.6	233.1	268.7
04T54C-92	188	7215	1.5	0.33749	4.8	0.04883	1.1	0.24	307.3	3.4	295.3	12.3	200.8	108.1
04T54C-47	148	8494	1.2	0.38589	5.9	0.05050	2.6	0.44	345.5	8.8	331.4	16.6	233.4	121.7
04T54C-15	70	3537	0.8	0.40017	5.7	0.05628	3.6	0.64	353.0	12.5	341.8	16.6	266.4	100.6
04T54C-21	83	2117	0.7	4.6129	4.9	0.30837	3.1	0.62	1732.7	46.4	1751.6	41.0	1774.3	70.1
04T54C-36	194	69820	2.9	5.34097	1.9	0.33964	1.3	0.66	1884.9	20.5	1875.4	16.3	1864.9	25.8

Analysis	U (ppm)	206Pb	207Pb*	U/Th	235U	Isotopic ratios			Apparent ages (Ma)						Age of youngest cluster (Ma) (3+ analyses)	
						±	206Pb*	±	238U (%)	corr.	206Pb*	±	235U (Ma)	207Pb* (Ma)	±	
041T54C-17	13	4036	7.1	5.38941	3.2	0.34202	2.3	0.72	1896.4	37.5	1883.2	27.2	1868.6	39.9	1868.6	39.9
041T54C-81	27	9011	1.7	5.43356	2	0.34217	1.4	0.67	1897.1	22.5	1890.2	17.4	1882.5	26.9	1882.5	26.9
041T54C-51	152	33547	0.7	5.57333	3.2	0.35044	2.5	0.77	1936.7	41.0	1912.0	27.3	1885.3	36.0	1885.3	36.0
041T54C-74	60	19535	0.4	5.70733	1.7	0.35879	1.3	0.8	1976.4	22.5	1932.5	14.3	1885.7	18.1	1885.7	18.1
041T54C-91	55	17986	0.9	5.34799	1.9	0.33363	1.6	0.82	1856.0	25.5	1876.6	16.5	1899.5	19.7	1899.5	19.7
041T54C-16	120	36848	0.7	5.49328	1.8	0.34132	1.3	0.73	1893.0	21.5	1899.5	15.5	1906.7	22.3	1906.7	22.3
041T54C-107	50	13322	0.7	5.60823	2	0.3484	1.3	0.66	1926.9	22.2	1917.4	17.5	1907.0	27.5	1907.0	27.5
041T54C-66	89	24085	1.3	5.50151	1.4	0.34115	1	0.71	1892.2	16.4	1900.8	12.2	1910.2	18.0	1910.2	18.0
041T54C-53	211	54577	1.3	5.596	1.5	0.34689	1	0.69	1919.7	16.6	1915.5	12.6	1910.9	19.0	1910.9	19.0
041T54C-61	253	59316	3.6	5.49126	1.5	0.33987	1	0.65	1886.0	16.4	1899.2	13.2	1913.7	21.0	1913.7	21.0
041T54C-69	400	92351	0.7	5.65437	1.4	0.34991	1	0.71	1934.2	16.7	1924.4	12.2	1913.9	17.9	1913.9	17.9
041T54C-27	352	101741	5.2	5.65147	2.6	0.34908	2.4	0.92	1930.2	39.3	1924.0	22.1	1917.3	17.9	1917.3	17.9
041T54C-78	215	44550	2.7	5.91397	1.8	0.36533	1.1	0.6	2007.2	18.2	1963.3	15.3	1917.3	25.3	1917.3	25.3
041T54C-63	156	38197	0.4	5.50181	1.8	0.33975	1	0.56	1885.5	16.3	1900.9	15.2	1917.7	26.2	1917.7	26.2
041T54C-84	227	46880	2	5.54847	3.9	0.34226	3.5	0.88	1897.6	57.4	1908.1	34.0	1919.7	33.0	1919.7	33.0
041T54C-59	302	80428	3.3	5.59686	2.1	0.34508	1.5	0.73	1911.1	25.5	1915.6	18.1	1920.5	25.6	1920.5	25.6
041T54C-58	90	15719	0.4	4.87467	4.8	0.30022	4.4	0.92	1692.4	65.3	1797.9	40.2	1922.5	33.7	1922.5	33.7
041T54C-75	240	35094	0.6	5.60915	1.5	0.34535	1.1	0.75	1912.4	19.0	1917.5	13.1	1923.1	17.9	1923.1	17.9
041T54C-95	149	42141	11.2	5.62827	1.6	0.34622	1.1	0.7	1916.5	18.7	1920.4	13.9	1924.7	20.6	1924.7	20.6
041T54C-29	207	33205	1.6	5.22522	1.4	0.32122	1	0.71	1795.7	15.7	1856.7	12.1	1925.8	18.0	1925.8	18.0
041T54C-72	205	42482	1.3	5.69799	1.5	0.35003	1	0.66	1934.7	16.7	1931.1	13.2	1927.1	20.6	1927.1	20.6
041T54C-77	2014	96175	3.4	5.62885	3.8	0.34557	3.6	0.96	1913.4	60.4	1920.5	32.9	1928.2	19.9	1928.2	19.9
041T54C-22	182	60260	1.1	5.73505	1.5	0.35192	1	0.67	1943.7	17.3	1936.7	13.3	1929.1	20.4	1929.1	20.4
041T54C-28	178	40116	0.3	5.71353	2.1	0.35048	1.3	0.65	1936.9	22.4	1933.4	17.9	1929.7	28.3	1929.7	28.3
041T54C-33	1043	190411	9	6.04706	1.6	0.36955	1.2	0.75	2027.3	20.8	1982.6	13.8	1936.4	18.6	1936.4	18.6
041T54C-76	694	183934	7.1	5.86891	1.8	0.35852	1	0.58	1975.2	17.5	1956.6	15.5	1937.1	26.1	1937.1	26.1
041T54C-14	659	172165	309	5.63543	1.9	0.34418	1	0.53	1906.8	16.5	1921.5	16.3	1937.5	28.8	1937.5	28.8
041T54C-35	210	38281	2.6	5.80444	2.3	0.35445	1.6	0.7	1955.8	26.7	1947.1	19.6	1937.8	29.0	1937.8	29.0
041T54C-55	166	44067	2.9	5.93748	2.1	0.36219	1.9	0.88	1992.5	32.2	1966.7	18.5	1939.7	17.9	1939.7	17.9
041T54C-57	714	180781	10.9	5.53125	2.8	0.33709	1.8	0.63	1872.7	28.9	1905.5	24.5	1941.4	39.7	1941.4	39.7
041T54C-62	618	18666	4.6	4.55203	2.2	0.2773	1.8	0.85	1577.7	25.7	1740.5	18.0	1942.1	20.5	1942.1	20.5
041T54C-73	47	21197	4	5.76243	1.5	0.35053	1	0.68	1937.1	16.7	1940.8	12.7	1944.7	19.1	1944.7	19.1
041T54C-85	635	49694	3.7	5.87934	1.6	0.3574	1.3	0.78	1969.8	21.6	1958.2	14.2	1945.9	18.3	1945.9	18.3
041T54C-82	1240	196821	6.1	5.72581	1.4	0.34749	1	0.71	1922.6	16.6	1935.3	12.2	1948.8	17.9	1948.8	17.9
041T54C-37	440	117509	3.6	5.69273	1.9	0.34528	1	0.53	1912.0	16.5	1930.3	16.3	1949.9	28.6	1949.9	28.6
041T54C-62	213	49255	0.8	5.63135	2.8	0.34137	1.5	0.55	1893.3	25.4	1920.9	24.2	1950.9	41.8	1950.9	41.8
041T54C-89	143	40118	1.8	5.91648	1.4	0.35854	1	0.71	1975.2	17.0	1963.7	12.3	1951.5	17.9	1951.5	17.9
041T54C-104	651	154385	19.7	5.42609	3.3	0.32879	3.1	0.93	1832.5	49.3	1889.0	28.5	1951.6	22.0	1951.6	22.0
041T54C-110	387	78118	2.3	5.5892	3.4	0.33477	3.2	0.96	1861.4	52.3	1904.9	29.1	1952.5	17.9	1952.5	17.9
041T54C-87	244	80959	3	5.52726	1.9	0.34245	1	0.71	1898.4	16.4	1924.8	12.2	1953.2	17.9	1953.2	17.9
041T54C-54	130	22320	1	5.65663	1.4	0.34245	1	0.71	1900.3	16.5	1926.1	14.1	1954.0	23.0	1954.0	23.0
041T54C-64	145	38790	3.7	5.66546	1.6	0.34283	1	0.61	1900.3	16.5	1926.1	14.1	1954.0	23.0	1954.0	23.0
041T54C-86	138	45098	5	5.58615	4.4	0.33777	4	0.9	1875.9	64.7	1914.0	37.9	1955.4	33.9	1955.4	33.9
041T54C-104	651	154385	10.1	5.8017	2	0.35059	1.3	0.67	1937.4	22.2	1946.7	17.1	1956.5	26.1	1956.5	26.1
041T54C-110	387	107019	2.1	6.21835	2.2	0.36877	1.6	0.71	2023.6	27.8	2007.0	19.7	1990.0	28.1	1990.0	28.1
041T54C-20	98	41331	4	5.86506	2.8	0.3477	2.4	0.86	1923.6	40.0	1956.1	24.2	1990.6	25.1	1990.6	25.1
041T54C-83	763	44320	3.9	5.76398	2.6	0.34127	2.4	0.92	1892.8	39.5	1941.0	22.5	1992.9	17.8	1992.9	17.8
041T54C-108	654	83562	29.8	6.06145	2.9	0.35756	2.5	0.85	1970.6	41.9	1984.7	25.2	1999.4	26.8	1999.4	26.8

Analysis	U (ppm)	206Pb	U/Th	207Pb*	Isotopic ratios				Apparent ages (Ma)				Age of youngest cluster (Ma) (3+ analyses)	
					235U (%)	238U (%)	206Pb* ±	error corr.	206Pb* (Ma)	235U (Ma)	207Pb* ±	206Pb* (Ma)		
041T54C-96	533	142244	4	6.13206	1.4	0.36073	1	0.71	1985.6	17.1	1994.8	12.3	2004.3	17.8
041T54C-12	198	62275	3	6.14509	2.6	0.36129	2.2	0.86	1988.3	38.0	1996.7	22.5	2005.3	22.9
041T54C-38	315	84250	13.6	6.26682	1.7	0.36838	1	0.58	2021.8	17.4	2013.8	15.0	2005.7	24.7
041T54C-1	219	34558	0.9	6.04867	2.3	0.35478	1.7	0.72	1957.4	28.0	1982.9	20.2	2009.6	28.8
041T54C-31	407	100786	1	6.31618	1.8	0.36984	1.3	0.74	2028.6	23.1	2012.7	15.8	2012.6	21.6
041T54C-41	53	16551	1.4	6.26338	1.5	0.3665	1	0.65	2012.9	17.3	2013.3	13.5	2013.8	20.8
041T54C-93	67	19702	1.9	6.29086	1.8	0.36626	1.4	0.76	2011.8	23.6	2017.2	15.8	2022.7	20.9
041T54C-2	160	35353	2.1	6.09983	1.9	0.35388	1	0.51	1953.1	16.8	1990.2	17.0	2029.0	29.6
041T54C-109	72	18343	1.5	6.08381	2.9	0.35268	2.2	0.75	1947.4	36.5	1987.9	25.3	2030.4	34.0
041T54C-23	282	52292	1.5	6.55897	2.1	0.37706	1.8	0.84	2062.5	31.9	2052.5	18.9	2042.4	20.5
041T54C-3	390	47477	0.7	6.08557	4.3	0.34946	3.9	0.91	1932.0	65.3	1988.2	37.3	2047.1	30.8
041T54C-99	205	36270	1.4	6.52273	1.6	0.37384	1	0.62	2047.4	17.5	2049.0	14.3	2050.5	22.6
041T54C-39	143	36171	2.7	6.31114	5.5	0.36162	4.7	0.86	1989.8	81.0	2020.0	48.1	2051.0	49.1
041T54C-94	61	19115	3	6.647	2.4	0.37944	1.9	0.8	2073.7	34.0	2065.6	21.3	2057.6	25.8
041T54C-19	157	22177	1.6	6.18013	1.7	0.35135	1.2	0.71	1942.0	20.8	2001.6	15.2	2063.8	21.5
041T54C-52	142	5486	1.4	6.45283	2	0.36657	1.5	0.73	2013.2	25.5	2039.5	17.8	2066.1	24.6
041T54C-26	693	208871	3.1	6.74265	2.3	0.37495	1.8	0.8	2052.7	32.2	2078.2	20.3	2103.6	24.2
041T54C-4	113	38241	1	7.29652	5.3	0.39418	4.8	0.92	2142.2	88.4	2148.4	47.1	2154.3	36.0
041T54C-65	37	13233	1.2	8.46132	2.1	0.42133	1.4	0.68	2267.4	27.3	2281.8	19.0	2294.7	26.2
041T54C-106	466	40398	1.7	9.98626	2.1	0.44669	1.8	0.88	2381.5	36.8	2430.7	19.4	2472.2	16.9
041T54C-79	422	89091	1.5	9.5568	3.8	0.42141	3.4	0.91	2266.9	65.4	2393.0	34.8	2502.2	26.9
041T54C-70	70	28991	2.4	10.55296	2.6	0.44307	2	0.74	2364.4	38.7	2466.9	24.5	2552.4	29.8
041T54C-103	117	46056	1	12.52672	3.2	0.50504	1.9	0.6	2637.0	41.9	2644.7	30.6	2650.7	43.3
041T54C-42	518	125773	1.8	12.59685	2.4	0.50469	2	0.81	2633.9	42.9	2650.0	23.0	2662.3	23.7
041T54C-90	132	56379	1.7	12.90989	2.6	0.50141	1.7	0.66	2619.9	36.5	2673.1	24.2	2713.6	31.8
041T54C-9	613	180815	0.7	13.74048	4.8	0.51406	4.4	0.92	2673.9	96.4	2732.0	45.1	2775.2	29.7
041T54C-60	88	22019	1.1	13.68398	2.2	0.51168	1.6	0.76	2663.8	35.8	2728.1	20.5	2776.0	23.2
041T54C-34	131	57740	0.8	16.90101	4.6	0.58272	4.2	0.91	2959.8	98.9	2929.2	43.8	2908.3	30.1

**Sample ELM 03 CH 24.3A**

ELM03CH243A-96	1024	3488	0.9	0.18989	15.48	0.02688	8.72	0.56	171	15	177	25	252	147	171	15
ELM03CH243A-21	140	836	1.6	0.21714	25.48	0.02846	3.37	0.13	181	6	200	45	426	282	181	6
ELM03CH243A-51	266	2572	0.9	0.20842	29.46	0.02954	6.06	0.21	188	11	192	50	248	332	188	11
ELM03CH243A-81	126	284	1.1	0.10099	63.41	0.03119	7.44	0.12	198	15	98	57	-1987	1176	198	15
ELM03CH243A-75	580	1370	1.2	0.24756	17.04	0.03138	5.25	0.31	210	11	225	34	376	182	210	11
ELM03CH243A-31	172	1756	1.8	0.24925	24.25	0.03345	4.38	0.18	212	9	226	48	373	269	212	9
ELM03CH243A-2	118	982	1.2	0.30607	22.79	0.03792	5.98	0.26	240	14	271	53	550	240	240	14
ELM03CH243A-53	216	496	0.3	0.25396	37.67	0.03995	2.68	0.07	253	7	230	75	3	453	253	7
ELM03CH243A-69	228	2740	0.9	0.31699	13.91	0.04097	3.86	0.28	259	10	280	33	457	148	259	10
ELM03CH243A-92	414	1302	1.6	0.30552	20.12	0.04155	1.58	0.08	262	4	271	47	343	227	262	4
ELM03CH243A-70	358	2810	1.2	0.31783	18.31	0.04253	3.09	0.17	269	8	280	44	379	203	269	8
ELM03CH243A-32	950	2356	0.9	0.33662	1.122	0.04293	1.9	0.17	271	5	295	28	487	122	271	5
ELM03CH243A-77	404	1890	0.9	0.33764	17.33	0.04334	1.23	0.07	274	3	295	44	472	191	274	3
ELM03CH243A-100	260	1528	1.3	0.33919	23.45	0.04364	5.21	0.22	275	14	297	59	467	253	275	14
ELM03CH243A-13	196	580	1.2	0.33911	28.39	0.04445	4.08	0.14	280	11	297	71	426	313	280	11
ELM03CH243A-52	336	1212	0.6	0.30714	21.33	0.0447	3.15	0.15	282	9	272	50	187	246	282	9
ELM03CH243A-4	394	1308	1	0.30909	18.99	0.04516	2.7	0.14	285	8	274	45	178	219	285	8
ELM03CH243A-95	110	2322	0.8	0.29086	22.58	0.04536	3.96	0.18	286	11	259	50	24	267	286	11
ELM03CH243A-97	152	818	0.5	0.30999	26.51	0.04594	4.63	0.17	290	13	274	62	145	306	290	13
ELM03CH243A-29	312	1518	1.2	0.3402	17.97	0.04636	4.11	0.23	292	12	297	45	338	198	292	12

182 (4)

Analysis	U (ppm)	206Pb	207Pb*	U/Th	235U	238U	206Pb*	±	Isotopic ratios			Apparent ages (Ma)				Age of youngest cluster (Ma) (3+ analyses)
									corr.	error	206Pb*	±	238U	(Ma)	235U	(Ma)
ELM03CH243A-11	50	1706	1.8	0.30861	20.44	0.04791	3.05	0.15	302	9	273	48	35	242	302	9
ELM03CH243A-50	612	2598	1.4	0.59243	9.32	0.04869	5.47	0.59	307	16	472	35	1388	72	307	16
ELM03CH243A-78	96	468	0.6	0.36545	31.56	0.04938	3.89	0.12	311	12	316	82	357	353	311	12
ELM03CH243A-30	194	1140	1.3	0.39206	18.72	0.05031	2.07	0.11	316	6	336	52	473	206	316	6
ELM03CH243A-61	166	2826	0.9	0.39985	1.563	0.05127	2.87	0.18	322	9	342	44	475	170	322	9
ELM03CH243A-7	538	1194	1.7	0.39422	17.49	0.05267	2.8	0.16	331	9	337	49	383	194	331	9
ELM03CH243A-46	236	944	0.8	0.4177	24.06	0.05287	2.05	0.09	332	7	354	70	503	264	332	7
ELM03CH243A-58	60	1506	0.9	0.43175	30.28	0.05468	4.69	0.15	343	16	364	89	502	329	343	16
ELM03CH243A-55	264	1368	0.9	0.45034	17.65	0.05608	1.94	0.11	381	7	378	54	359	198	381	7
ELM03CH243A-80	264	1870	0.8	0.48374	14.36	0.06089	4.48	0.31	381	17	401	47	515	150	381	17
ELM03CH243A-37	154	1032	1.8	0.64167	24.51	0.06098	4.42	0.18	382	16	503	93	1104	241	382	16
ELM03CH243A-10	80	1010	1	0.49822	34.65	0.06478	3.66	0.11	405	14	411	111	444	383	405	14
ELM03CH243A-41	260	1234	1.3	0.53467	20.7	0.06705	3.63	0.18	412	15	435	71	558	222	412	15
ELM03CH243A-90	30	1414	1	0.48738	28.17	0.06705	4.84	0.17	418	20	403	90	317	315	418	20
ELM03CH243A-43	176	2866	0.9	0.52126	10.77	0.06855	4.3	0.4	427	18	426	37	418	110	427	18
ELM03CH243A-17	170	804	1.4	0.63693	26.17	0.07014	7.61	0.29	437	32	500	99	802	262	437	32
ELM03CH243A-20	146	1608	1	0.49624	21.35	0.07244	7.03	0.33	451	31	409	70	180	235	451	31
ELM03CH243A-64	144	1872	1	0.5286	16.81	0.07474	3.31	0.2	465	15	431	57	254	189	465	15
ELM03CH243A-42	306	3516	1.4	0.62803	9.91	0.07854	2.82	0.28	487	13	495	38	530	104	487	13
ELM03CH243A-62	54	2242	0.9	0.773	17.59	0.09808	4.28	0.24	603	25	582	75	498	188	603	25
ELM03CH243A-68	108	2926	1	0.8703	15.55	0.10757	4.07	0.26	659	25	636	71	555	164	659	25
ELM03CH243A-91	204	2204	0.8	1.05728	10.42	0.12111	2.1	0.2	737	15	733	53	719	108	737	15
ELM03CH243A-14	76	1504	3	4.67207	7.88	0.30226	2.24	0.28	1703	33	1762	64	1834	68	1834	68
ELM03CH243A-83	118	2552	1.4	4.86933	5.37	0.3123	2	0.37	1752	31	1797	44	1850	45	1850	45
ELM03CH243A-85	182	5074	1.2	5.02003	3.43	0.32025	1.68	0.49	1791	26	1823	29	1859	27	1859	27
ELM03CH243A-59	322	9792	2.4	5.02315	4.22	0.32034	3.66	0.87	1791	57	1823	35	1860	19	1860	19
ELM03CH243A-93	96	2200	0.9	5.27957	7.28	0.33653	2.78	0.38	1870	45	1866	60	1861	61	1861	61
ELM03CH243A-65	318	9166	3	4.63488	4.36	0.29326	4	0.92	1658	58	1756	36	1874	16	1874	16
ELM03CH243A-99	164	5764	4	5.16669	5.37	0.32637	3.08	0.57	1821	49	1847	45	1877	40	1877	40
ELM03CH243A-6	104	1284	1.1	5.17645	8.6	0.32499	2.86	0.33	1814	45	1849	71	1888	73	1888	73
ELM03CH243A-74	118	3520	1.5	5.37813	4.04	0.33692	1.58	0.39	1872	26	1881	34	1892	33	1892	33
ELM03CH243A-94	48	1406	1	5.40793	9.26	0.30569	4.28	0.46	1725	65	1804	75	1895	74	1895	74
ELM03CH243A-79	970	23056	2.7	5.44981	1.82	0.33993	1.7	0.93	1886	28	1893	16	1900	6	1900	6
ELM03CH243A-23	156	2632	8.7	4.42851	8.4	0.27508	6.94	0.83	1567	96	1718	67	1907	42	1907	42
ELM03CH243A-16	1050	19658	1.2	5.12593	1.91	0.31819	1.78	0.93	1781	28	1840	16	1908	6	1908	6
ELM03CH243A-87	160	5812	0.8	5.55389	4.46	0.34472	2.66	0.6	1909	44	1909	38	1909	32	1909	32
ELM03CH243A-25	196	4826	2	5.50381	3.46	0.34135	2.1	0.61	1893	34	1901	29	1910	25	1910	25
ELM03CH243A-3	218	2888	1.7	4.85632	4.78	0.30105	2.73	0.57	1697	41	1795	40	1911	35	1911	35
ELM03CH243A-56	352	12366	2	5.35095	6.52	0.3312	6.25	0.96	1844	100	1877	54	1914	17	1914	17
ELM03CH243A-38	538	15976	2.4	5.38395	4.22	0.33224	3.73	0.88	1849	60	1882	36	1919	18	1919	18
ELM03CH243A-16	1280	13312	1	5.41866	4.1	0.33201	1.89	0.46	1848	30	1888	35	1932	33	1932	33
ELM03CH243A-57	126	4486	1.9	5.55255	5.14	0.34034	3.27	0.64	1888	53	1905	43	1922	36	1922	36
ELM03CH243A-84	190	6650	1.8	5.41156	3.12	0.33336	1.63	0.52	1855	26	1887	26	1922	24	1922	24
ELM03CH243A-44	142	3450	4.6	4.80843	5.44	0.29565	3.23	0.59	1670	47	1786	45	1926	39	1926	39
ELM03CH243A-67	366	12380	4.3	5.61462	2.36	0.34513	1.92	0.81	1911	32	1918	20	1926	12	1926	12
ELM03CH243A-15	158	3312	1	5.41866	4.1	0.33201	1.89	0.46	1848	30	1888	35	1932	33	1932	33
ELM03CH243A-45	154	4904	0.6	5.38036	4.2	0.32948	2.72	0.65	1836	43	1882	35	1933	29	1933	29
ELM03CH243A-73	600	20008	16.1	5.78298	2.3	0.35385	2.16	0.94	1953	36	1944	20	1934	7	1934	7
ELM03CH243A-34	300	10310	3.1	5.63477	4.83	0.34311	4.44	0.92	1902	73	1921	41	1943	17	1943	17
ELM03CH243A-19	162	4282	2.9	5.05336	6.45	0.30703	5.12	0.79	1726	77	1828	53	1947	35	1947	35
ELM03CH243A-47	476	13812	1.8	5.62687	2.97	0.34018	2.78	0.94	1888	45	1920	25	1956	9	1956	9

Analysis	U (ppm)	206Pb	204Pb	235U	207Pb*	U/Th	Isotopic ratios			Apparent ages (Ma)						Age of youngest cluster (Ma) (3+ analyses)	
							±	206Pb*	238U	error	206Pb*	235U	207Pb*	207Pb*	207Pb*	Best age	
ELM03CH243A-18	286	3600	2,1	5,11253	7,33	0,1430	21,1	0,0234	1,4	0,07	148,8	2,1	135,7	26,9	-87,8	522,0	148,8 2,1
ELM03CH243A-5	492	8480	7	5,67884	3,85	0,34227	3,48	0,91	1735	100	1838	60	1958	28	1958	28	
ELM03CH243A-63	528	9956	1,8	5,48815	3,53	0,33072	3,27	0,93	1842	52	1899	30	1961	15	1961	15	
ELM03CH243A-49	456	10000	2	5,87088	3,25	0,35327	2,92	0,9	1950	49	1957	28	1964	13	1964	13	
ELM03CH243A-71	158	3858	1,9	5,7006	6,32	0,34105	2,13	0,34	1892	35	1932	53	1974	53	1974	53	
ELM03CH243A-48	322	5968	1,7	5,46387	3,59	0,32621	2,7	0,75	1820	43	1895	30	1978	21	1978	21	
ELM03CH243A-33	430	13414	3	5,30808	3,69	0,31668	3,45	0,94	1774	53	1870	31	1979	12	1979	12	
ELM03CH243A-8	114	1316	1,2	5,6822	8,12	0,33837	2,03	0,25	1879	33	1929	68	1983	70	1983	70	
ELM03CH243A-40	1288	3334	2,4	5,85089	4	0,34611	2,27	0,57	1916	38	1954	34	1994	29	1994	29	
ELM03CH243A-72	140	2110	0,9	5,71082	5,9	0,33572	3,23	0,55	1866	52	1933	50	2006	44	2006	44	
ELM03CH243A-35	296	10176	1	6,04796	3,56	0,35412	3,29	0,92	1954	55	1983	31	2013	12	2013	12	
ELM03CH243A-89	82	2956	1	6,22005	4,78	0,36368	1,75	0,37	2000	30	2007	41	2015	39	2015	39	
ELM03CH243A-12	176	3414	3,1	5,10503	5,37	0,29711	4,1	0,76	1677	60	1837	45	2023	31	2023	31	
ELM03CH243A-39	1016	15002	11,1	4,92149	2,85	0,28644	2,64	0,93	1624	38	1806	24	2023	9	2023	9	
ELM03CH243A-36	188	4672	3,3	5,28442	4,54	0,30491	3,8	0,84	1716	57	1866	38	2039	22	2039	22	
ELM03CH243A-82	52	2770	1,6	5,89094	11,4	0,33516	5,92	0,52	1863	95	1960	94	2063	86	2063	86	
ELM03CH243A-66	622	12086	1,9	6,06841	3,72	0,322792	3,58	0,96	1828	57	1986	32	2154	9	2154	9	
ELM03CH243A-9	1306	23240	2,5	8,15079	2,52	0,39683	2,46	0,98	2154	45	2248	23	2334	5	2334	5	
ELM03CH243A-86	158	5054	0,9	8,67659	3,82	0,41513	1,4	0,37	2238	26	2305	34	2364	30	2364	30	
ELM03CH243A-26	522	15458	2,3	8,90231	2,75	0,41859	2,64	0,96	2254	50	2328	25	2394	7	2394	7	
ELM03CH243A-27	156	9718	1,8	10,66818	4,16	0,47288	3,69	0,89	2495	76	2495	38	2495	16	2495	16	
ELM03CH243A-24	214	6112	1,3	11,10609	2,95	0,45376	2,52	0,86	2412	51	2532	27	2630	13	2630	13	
ELM03CH243A-54	172	7918	1,6	12,93918	2,79	0,51033	2,54	0,91	2658	55	2675	26	2688	9	2688	9	
ELM03CH243A-98	384	24534	1,4	14,00267	1,3	0,51326	1,19	0,91	2671	26	2750	12	2809	4	2809	4	
<b>Sample ELM06 PV10</b>																	
ELM06-PV10-44	113	936	0,6	0,1430	21,1	0,0234	1,4	0,07	148,8	2,1	135,7	26,9	-87,8	522,0	148,8 2,1		
ELM06-PV10-52	80	870	0,7	0,1554	21,1	0,0246	1,0	0,05	157,0	1,6	146,7	28,8	-16,6	513,7	157,0	1,6	
ELM06-PV10-43	289	2764	0,7	0,2017	5,9	0,0298	1,0	0,17	189,4	1,9	186,6	10,0	151,7	135,4	189,4	1,9	
ELM06-PV10-32	543	4594	3,0	0,2576	3,4	0,0354	1,7	0,49	224,2	3,7	232,7	7,1	320,0	67,3	224,2	3,7	
ELM06-PV10-94	439	6484	0,6	0,2604	2,9	0,0369	1,0	0,35	233,5	2,3	235,0	6,1	250,1	62,5	233,5	2,3	
ELM06-PV10-4	41	640	0,9	0,2361	29,2	0,0376	1,8	0,06	237,7	4,1	215,2	56,6	-23,9	717,9	237,7	4,1	
ELM06-PV10-12	95	1544	0,8	0,2708	11,3	0,0380	1,0	0,09	240,2	2,4	243,4	24,4	273,9	257,7	240,2	2,4	
ELM06-PV10-10	379	4190	0,6	0,2913	3,9	0,0400	1,2	0,30	252,6	2,9	259,6	9,0	322,8	85,3	252,6	2,9	
ELM06-PV10-29	211	2812	0,4	0,2946	3,5	0,0409	1,7	0,48	258,5	4,3	262,2	8,2	295,4	70,5	258,5	4,3	
ELM06-PV10-75	426	4774	9,4	0,3042	4,9	0,0413	1,5	0,30	261,1	3,8	269,7	11,5	345,0	105,2	261,1	3,8	
ELM06-PV10-60	118	2722	2,5	0,3183	10,8	0,0420	1,0	0,09	265,1	2,6	280,6	26,4	411,8	240,0	265,1	2,6	
ELM06-PV10-65	158	4030	1,1	0,2958	8,3	0,0423	1,0	0,12	267,0	2,6	263,1	19,2	229,0	189,9	267,0	2,6	
ELM06-PV10-90	137	2736	0,6	0,3207	11,7	0,0433	1,0	0,09	273,4	2,7	282,5	28,8	358,1	263,0	273,4	2,7	
ELM06-PV10-58	361	8506	0,9	0,3139	3,5	0,0441	1,0	0,29	278,5	2,7	277,2	8,5	266,2	76,9	278,5	2,7	
ELM06-PV10-85	84	2268	0,9	0,3167	8,3	0,0449	1,0	0,12	282,8	2,8	279,3	20,2	250,3	189,5	282,8	2,8	
ELM06-PV10-107	138	2904	1,3	0,3240	8,3	0,0449	1,1	0,13	282,8	3,1	285,0	20,6	302,4	187,9	282,8	3,1	
ELM06-PV10-2	159	2640	0,8	0,3070	7,4	0,0453	1,0	0,14	285,4	2,8	271,9	17,6	156,8	171,3	285,4	2,8	
ELM06-PV10-23	2413	30232	1,2	0,3307	1,8	0,0454	1,5	0,83	286,4	4,1	290,1	4,5	319,5	22,8	286,4	4,1	
ELM06-PV10-76	104	2960	2,0	0,3246	10,1	0,0468	2,0	0,20	295,1	5,8	285,4	25,2	207,1	231,0	295,1	5,8	
ELM06-PV10-89	179	3498	0,9	0,3388	5,9	0,0479	1,0	0,17	301,4	2,9	296,3	15,1	255,9	133,2	301,4	2,9	
ELM06-PV10-63	187	4448	0,7	0,3323	2,6	0,0483	1,0	0,38	304,1	3,0	326,3	4,0	190,3	56,4	304,1	3,0	
ELM06-PV10-28	420	6614	2,0	0,3867	3,1	0,0519	1,3	0,43	321,9	6,6	371,5	64,2	326,3	4,0	326,3	4,0	
ELM06-PV10-99	476	11318	4,4	0,3899	2,3	0,0531	1,0	0,43	334,3	3,2	334,3	6,6	339,9	47,6	333,5	3,2	
ELM06-PV10-100	887	19882	1,7	0,4305	1,8	0,0576	1,1	0,61	360,7	3,9	363,6	5,6	381,7	32,6	360,7	3,9	

Analysis	U (ppm)	206Pb	207Pb*	U/Th	207Pb*	Isotopic ratios			Apparent ages (Ma)					Age of youngest cluster (Ma) (3+ analyses)	
						235U (%)	238U (%)	error corr.	206Pb* ±	238U (Ma)	235U (Ma)	207Pb* ±	207Pb* (Ma)	Best age (Ma)	
ELM06-PV10-27	125	3326	0.7	0.4895	5.9	0.0636	1.0	0.17	397.3	3.9	404.5	19.8	445.8	1300	397.3
ELM06-PV10-54	409	12730	1.0	0.6152	2.0	0.0587	1.0	0.51	488.5	4.7	486.8	7.6	479.1	37.4	488.5
ELM06-PV10-73	248	11324	1.7	0.9552	3.3	0.1072	2.5	0.78	656.5	15.9	680.8	16.2	762.1	43.6	656.5
ELM06-PV10-14	139	7678	1.0	1.2117	2.1	0.1347	1.0	0.47	814.7	7.7	806.0	11.9	782.0	39.6	814.7
ELM06-PV10-15	73	9326	1.5	4.5542	2.0	0.3139	1.0	0.49	1760.0	15.4	1740.9	17.0	1718.1	32.8	1718.1
ELM06-PV10-49	174	17682	1.4	4.3284	1.5	0.2946	1.2	0.76	1664.7	17.0	1698.8	12.6	1741.1	18.3	1741.1
ELM06-PV10-71	485	71566	2.2	4.5526	1.4	0.3088	1.0	0.71	1734.7	15.2	1740.6	11.8	1747.7	18.3	1747.7
ELM06-PV10-102	64	9646	1.6	4.8273	1.8	0.3235	1.0	0.57	1806.8	15.8	1789.7	14.8	1769.8	26.5	1769.8
ELM06-PV10-31	325	44250	4.8	4.1064	1.4	0.2722	1.0	0.71	1551.9	13.8	1655.6	11.6	1789.8	18.2	1789.8
ELM06-PV10-104	516	59038	4.8	3.3511	2.1	0.2213	1.9	0.88	1288.8	22.1	1493.1	16.7	1796.4	18.2	1796.4
ELM06-PV10-62	499	22354	1.3	4.6849	1.4	0.3027	1.0	0.70	1704.5	15.0	1764.5	11.9	1836.4	18.4	1836.4
ELM06-PV10-93	166	20958	2.3	4.7637	1.4	0.3069	1.0	0.69	1725.5	15.1	1778.5	12.1	1841.3	18.8	1841.3
ELM06-PV10-13	274	36610	4.4	5.0939	1.5	0.3268	1.0	0.67	1822.6	15.9	1835.1	12.7	1849.2	20.1	1849.2
ELM06-PV10-42	547	47838	1.7	4.6642	1.4	0.2991	1.0	0.71	1686.9	14.8	1760.8	11.8	1849.7	18.1	1849.7
ELM06-PV10-6	169	17462	0.7	4.9533	1.4	0.3173	1.0	0.71	1776.8	15.5	1811.4	12.0	1851.5	18.1	1851.5
ELM06-PV10-7	141	16938	1.8	5.2286	1.4	0.3342	1.0	0.71	1858.9	16.1	1857.3	12.1	1855.5	18.1	1855.5
ELM06-PV10-9	817	56202	2.2	4.6366	2.0	0.2964	1.7	0.87	1673.2	25.6	1755.9	16.8	1855.7	18.1	1855.7
ELM06-PV10-97	218	25924	1.7	4.8678	2.2	0.3109	2.0	0.90	1745.3	30.7	1796.7	18.9	1856.9	18.1	1856.9
ELM06-PV10-96	92	11978	1.4	5.4363	1.4	0.3468	1.0	0.71	1919.2	16.6	1890.6	12.2	1859.4	18.1	1859.4
ELM06-PV10-48	1244	93874	38.2	3.8636	1.9	0.2464	1.7	0.86	1419.8	21.0	1606.1	15.6	1859.8	18.1	1859.8
ELM06-PV10-69	351	64826	3.3	5.2763	1.7	0.3365	1.4	0.81	1869.6	22.2	1865.0	14.5	1859.9	18.1	1859.9
ELM06-PV10-80	208	17570	1.6	5.1442	2.0	0.3278	1.7	0.87	1827.9	27.5	1843.4	17.0	1861.0	18.1	1861.0
ELM06-PV10-74	370	45274	8.1	5.2869	1.4	0.3361	1.0	0.71	1867.7	16.2	1866.8	12.1	1865.7	18.0	1865.7
ELM06-PV10-8	240	19818	2.7	4.9752	1.6	0.3158	1.0	0.61	1769.3	15.5	1815.1	13.9	1868.1	23.7	1868.1
ELM06-PV10-53	1988	132662	11.1	5.2762	1.4	0.3345	1.0	0.71	1860.0	16.2	1865.0	12.1	1870.6	18.0	1870.6
ELM06-PV10-11	193	27440	2.9	4.9262	1.5	0.3122	1.1	0.74	1751.4	16.9	1806.8	12.6	1871.2	18.1	1871.2
ELM06-PV10-98	321	33466	1.2	5.3288	1.4	0.3374	1.0	0.71	1874.1	16.3	1873.5	12.1	1872.8	18.0	1872.8
ELM06-PV10-67	442	54522	2.4	3.8737	2.2	0.2452	2.0	0.89	1413.9	25.1	1608.2	17.9	1872.9	18.0	1872.9
ELM06-PV10-46	386	41134	3.7	5.0959	1.4	0.3223	1.0	0.71	1801.0	15.7	1835.4	12.0	1874.7	18.0	1874.7
ELM06-PV10-56	81	15664	1.5	5.6775	2.2	0.3570	1.0	0.45	1968.0	17.0	1927.9	19.3	1885.2	36.0	1885.2
ELM06-PV10-105	124	15464	1.6	5.3651	1.4	0.3368	1.0	0.71	1871.3	16.2	1879.3	12.1	1888.1	18.0	1888.1
ELM06-PV10-84	63	12246	1.8	5.6213	2.1	0.3528	1.0	0.47	1947.9	16.8	1919.4	18.2	1888.7	33.4	1888.7
ELM06-PV10-39	482	51792	4.1	5.5862	1.5	0.3485	1.1	0.73	1927.5	17.8	1914.0	12.7	1899.3	18.2	1899.3
ELM06-PV10-109	31	4166	0.8	4.4519	3.2	0.2773	1.0	0.31	1577.6	14.0	1722.1	26.5	1902.4	54.5	1902.4
ELM06-PV10-55	747	88936	20.3	5.2803	2.0	0.3289	1.7	0.86	1832.9	27.4	1865.7	17.0	1902.4	18.0	1902.4
ELM06-PV10-66	233	44726	1.8	5.6422	1.4	0.3495	1.0	0.71	1932.2	16.7	1922.6	12.2	1912.2	18.0	1912.2
ELM06-PV10-64	27	4674	0.4	5.3058	5.0	0.3283	1.5	0.30	1830.1	23.6	1869.8	42.7	1914.2	85.6	1914.2
ELM06-PV10-18	221	6610	3.0	4.8975	1.5	0.3020	1.0	0.70	1701.3	15.6	1801.8	12.5	1920.2	18.8	1920.2
ELM06-PV10-91	513	76768	9.3	5.8901	1.4	0.3613	1.0	0.71	1988.4	17.1	1959.8	12.3	1929.7	17.9	1929.7
ELM06-PV10-88	153	10198	1.7	5.7817	1.4	0.3534	1.0	0.71	1950.6	16.8	1943.7	12.2	1936.3	17.9	1936.3
ELM06-PV10-78	204	33060	0.5	5.7938	1.5	0.3541	1.0	0.68	1954.0	16.9	1945.5	12.7	1936.4	19.2	1936.4
ELM06-PV10-61	290	15702	0.8	5.5751	1.4	0.3394	1.0	0.71	1883.7	16.3	1912.3	12.2	1943.4	17.9	1943.4
ELM06-PV10-30	349	39954	6.5	5.9546	2.8	0.3624	2.6	0.93	1993.4	44.8	1969.2	24.5	1943.9	19.0	1943.9
ELM06-PV10-91	513	76768	9.3	5.9067	1.4	0.3579	1.0	0.71	1972.0	17.0	1962.2	12.3	1951.9	17.9	1951.9
ELM06-PV10-33	1039	60146	27.7	5.4747	1.9	0.3300	1.1	0.56	1838.2	17.4	1896.6	16.6	1961.2	28.6	1961.2
ELM06-PV10-51	179	12994	1.0	5.8096	1.6	0.3491	1.0	0.61	1930.2	16.7	1947.8	14.2	1966.7	23.1	1966.7
ELM06-PV10-18	504	25992	1.3	4.1950	4.8	0.2515	4.7	0.98	1446.4	60.4	1673.0	39.1	1970.3	17.8	1970.3
ELM06-PV10-17	146	14868	1.9	4.7965	3.1	0.2865	3.0	0.95	1623.9	42.5	1784.3	26.3	1977.3	17.8	1977.3
ELM06-PV10-95	171	14568	19.7	6.3739	1.4	0.3775	1.0	0.71	2064.8	17.7	2028.7	12.4	1992.1	17.8	1992.1

Analysis	U (ppm)	206Pb	204Pb	207Pb*	235U	U/Th	207Pb*	Isotopic ratios			Apparent ages (Ma)				Age of youngest cluster (Ma) (3+ analyses)							
								±	206Pb*	±	238U	corr.	error	206Pb*	±	207Pb*	±	206Pb*	±	207Pb*	±	Best age
ELM06-PV10-83	181	32768	2.0	64376	1.4	0.3805	1.0	0.71	2078.6	17.8	2037.4	12.4	1996.0	17.8	1996.0	17.8	1996.0	17.8	1996.0	17.8	1996.0	17.8
ELM06-PV10-59	215	34980	1.7	63341	2.3	0.3728	1.9	0.82	2042.8	33.1	2023.2	20.1	2003.2	23.1	2003.2	23.1	2003.2	23.1	2003.2	23.1	2003.2	23.1
ELM06-PV10-110	409	71832	4.2	63629	1.4	0.3737	1.0	0.71	2046.7	17.5	2027.2	12.4	2007.3	17.7	2007.3	17.7	2007.3	17.7	2007.3	17.7	2007.3	17.7
ELM06-PV10-70	801	128676	11.8	62719	2.0	0.3678	1.6	0.82	2019.1	27.6	2014.5	17.1	2009.8	20.1	2009.8	20.1	2009.8	20.1	2009.8	20.1	2009.8	20.1
ELM06-PV10-81	187	12558	1.4	57386	2.1	0.3358	1.0	0.49	1866.4	16.2	1937.2	17.7	2013.8	31.8	2013.8	31.8	2013.8	31.8	2013.8	31.8	2013.8	31.8
ELM06-PV10-19	237	2182	1.2	57596	2.5	0.3369	1.0	0.39	1871.9	16.2	1940.4	22.0	2014.2	41.4	2014.2	41.4	2014.2	41.4	2014.2	41.4	2014.2	41.4
ELM06-PV10-106	190	30720	2.2	65036	1.9	0.3798	1.6	0.85	2075.4	28.2	2046.4	16.5	2017.2	17.7	2017.2	17.7	2017.2	17.7	2017.2	17.7	2017.2	17.7
ELM06-PV10-82	181	37350	2.8	66589	1.7	0.3860	1.0	0.58	2104.1	18.0	2067.2	15.1	2030.5	24.6	2030.5	24.6	2030.5	24.6	2030.5	24.6	2030.5	24.6
ELM06-PV10-68	239	46748	3.7	65077	1.4	0.3765	1.0	0.71	2060.0	17.6	2046.9	12.4	2033.8	17.7	2033.8	17.7	2033.8	17.7	2033.8	17.7	2033.8	17.7
ELM06-PV10-24	340	27980	2.9	59941	1.4	0.3454	1.0	0.71	1912.5	16.5	1975.0	12.3	2041.0	17.7	2041.0	17.7	2041.0	17.7	2041.0	17.7	2041.0	17.7
ELM06-PV10-57	110	19930	4.0	60966	2.5	0.3471	1.0	0.40	1920.5	16.6	1989.8	21.9	2062.5	40.6	2062.5	40.6	2062.5	40.6	2062.5	40.6	2062.5	40.6
ELM06-PV10-77	54	8132	1.0	63750	4.4	0.3602	1.0	0.23	1982.9	17.1	2028.8	39.0	2075.9	76.1	2075.9	76.1	2075.9	76.1	2075.9	76.1	2075.9	76.1
ELM06-PV10-20	181	1870	1.2	64914	3.7	0.3626	1.0	0.27	1994.6	17.2	2044.7	32.8	2095.7	63.1	2095.7	63.1	2095.7	63.1	2095.7	63.1	2095.7	63.1
ELM06-PV10-101	201	35400	2.4	78952	1.9	0.3952	1.0	0.52	2147.0	18.3	2216.5	17.5	2281.3	28.6	2281.3	28.6	2281.3	28.6	2281.3	28.6	2281.3	28.6
ELM06-PV10-22	283	42784	10.2	91304	3.2	0.4229	1.0	0.31	2273.7	19.2	2351.2	29.6	2419.1	52.1	2419.1	52.1	2419.1	52.1	2419.1	52.1	2419.1	52.1
ELM06-PV10-3	186	29358	2.0	128383	1.5	0.5144	1.0	0.66	2675.5	21.9	2667.9	14.4	2662.0	19.1	2662.0	19.1	2662.0	19.1	2662.0	19.1	2662.0	19.1
ELM06-PV10-41	158	25114	2.6	132670	1.4	0.5182	1.0	0.71	2691.6	22.0	2698.8	13.4	2704.3	16.5	2704.3	16.5	2704.3	16.5	2704.3	16.5	2704.3	16.5
ELM06-PV10-79	115	25714	1.2	141409	1.4	0.5467	1.0	0.71	2811.5	22.8	2759.2	13.4	2721.1	16.5	2721.1	16.5	2721.1	16.5	2721.1	16.5	2721.1	16.5
ELM06-PV10-40	74	16256	1.0	137029	1.5	0.5288	1.0	0.71	2736.3	23.0	2729.4	13.8	2724.3	17.0	2724.3	17.0	2724.3	17.0	2724.3	17.0	2724.3	17.0
ELM06-PV10-35	126	33446	1.6	137975	1.4	0.5295	1.0	0.71	2739.2	22.3	2735.9	13.4	2733.4	16.5	2733.4	16.5	2733.4	16.5	2733.4	16.5	2733.4	16.5
ELM06-PV10-16	62	12028	2.5	138501	1.6	0.5304	1.0	0.62	2743.1	22.3	2739.5	15.3	2736.9	20.9	2736.9	20.9	2736.9	20.9	2736.9	20.9	2736.9	20.9
ELM06-PV10-108	238	43974	2.0	143899	1.4	0.5500	1.0	0.71	2825.3	22.9	2775.8	13.4	2739.9	16.5	2739.9	16.5	2739.9	16.5	2739.9	16.5	2739.9	16.5
ELM06-PV10-21	175	36414	2.4	137818	1.4	0.5219	1.0	0.71	2707.1	22.1	2734.1	13.4	2755.4	16.4	2755.4	16.4	2755.4	16.4	2755.4	16.4	2755.4	16.4
ELM06-PV10-86	205	56490	2.6	144808	1.4	0.5458	1.0	0.71	2807.6	22.8	2781.7	13.4	2763.0	16.4	2763.0	16.4	2763.0	16.4	2763.0	16.4	2763.0	16.4
ELM06-PV10-45	884	118846	3.6	152168	1.4	0.5602	1.0	0.71	2867.6	23.1	2828.9	13.5	2801.5	16.4	2801.5	16.4	2801.5	16.4	2801.5	16.4	2801.5	16.4
<b>Sample 53.1 Stobolvoi Island</b>																		155 (4)				
53102-21	504	8350	0.8	0.15687	4.6	0.02408	2.0	0.42	153.4	3.0	148.0	6.4	61.5	100.4	153.4	3.0	153.4	3.0	153.4	3.0	153.4	3.0
53102-63	651	10930	4.1	0.16040	4.1	0.02441	2.4	0.58	155.5	3.7	151.0	5.8	82.4	79.6	155.5	3.7	155.5	3.7	155.5	3.7	155.5	3.7
53102-56	117	2468	0.6	0.16190	7.6	0.02454	3.1	0.40	156.3	4.7	152.4	10.8	91.4	165.5	156.3	4.7	156.3	4.7	156.3	4.7	156.3	4.7
53102-109	70	1504	1.4	0.16289	33.5	0.02514	3.7	0.11	160.1	5.9	153.2	47.7	49.0	814.9	160.1	5.9	160.1	5.9	160.1	5.9	160.1	5.9
53102-22	505	6128	0.4	0.23587	5.1	0.03547	1.5	0.30	224.7	3.4	215.0	9.9	110.6	114.4	224.7	3.4	224.7	3.4	224.7	3.4	224.7	3.4
53102-48	178	4229	0.8	0.23608	7.9	0.03629	1.5	0.19	229.8	3.4	215.2	15.4	58.6	185.9	229.8	3.4	229.8	3.4	229.8	3.4	229.8	3.4
53102-43	32	1153	0.6	0.24247	23.5	0.03736	4.9	0.21	236.4	11.3	220.4	46.6	52.9	555.1	236.4	11.3	236.4	11.3	236.4	11.3	236.4	11.3
53102-105	253	5726	0.7	0.27269	4.6	0.03789	2.6	0.56	239.8	6.0	244.8	10.0	293.8	87.3	239.8	87.3	239.8	87.3	239.8	87.3	239.8	87.3
53102-28	185	4550	0.5	0.27043	5.4	0.03813	1.2	0.22	241.2	4.5	241.2	5.6	241.1	40.3	241.2	4.5	241.2	4.5	241.2	4.5	241.2	4.5
53102-68	503	20193	2.0	0.266818	2.6	0.03813	1.9	0.74	241.2	4.5	241.2	5.6	241.1	40.3	241.2	4.5	241.2	4.5	241.2	4.5	241.2	4.5
53102-8	175	2615	0.3	0.25736	6.4	0.03851	3.7	0.58	243.6	8.8	232.5	13.2	122.0	122.6	243.6	8.8	243.6	8.8	243.6	8.8	243.6	8.8
53102-80	304	9190	0.7	0.27703	2.5	0.03982	1.5	0.61	251.7	3.8	248.3	5.6	215.8	46.8	251.7	3.8	251.7	3.8	251.7	3.8	251.7	3.8
53102-19	691	17334	0.3	0.28613	1.4	0.04074	1.0	0.69	257.4	2.5	255.5	3.3	237.8	24.2	257.4	2.5	257.4	2.5	257.4	2.5	257.4	2.5
53102-17	217	6786	0.8	0.29526	4.4	0.04083	1.2	0.28	258.0	3.1	262.7	10.1	304.8	95.4	258.0	3.1	258.0	3.1	258.0	3.1	258.0	3.1
53102-86	239	6338	0.9	0.27959	4.0	0.04097	1.2	0.30	258.9	3.0	250.3	8.9	171.2	89.5	258.9	3.0	258.9	3.0	258.9	3.0	258.9	3.0
53102-33	292	6893	1.7	0.29248	3.8	0.04229	2.5	0.64	267.0	6.5	260.5	8.8	202.4	67.9	267.0	6.5	267.0	6.5	267.0	6.5	267.0	6.5
53102-50	74	1763	0.5	0.29202	5.9	0.04266	3.2	0.55	269.3	8.4	260.1	13.5	178.7	114.7	269.3	8.4	269.3	8.4	269.3	8.4	269.3	8.4
53102-85	23	526	0.5	0.27706	24.9	0.04280	6.1	0.25	270.2	16.2	248.3	54.8	46.8	582.9	270.2	16.2	270.2	16.2	270.2	16.2	270.2	16.2
53102-72	122	2680	0.3	0.28352	9.9	0.04335	2.5	0.25	274.8	6.8	253.4	22.3	60.4	229.2	274.8	6.8	274.8	6.8	274.8	6.8</td		

Analysis	U (ppm)	206Pb	207Pb*	U/Th	235U	±	206Pb*	±	Isotopic ratios				Apparent ages (Ma)				Age of youngest cluster (Ma) (3+ analyses)
									238U (%)	corr.	206Pb* error	238U (Ma)	235U (Ma)	207Pb* ±	207Pb* (Ma)	Best age (Ma)	±
53102-31	152	4194	0.4	0.31276	5.2	0.04561	2.1	0.40	287.5	5.8	276.3	12.6	182.4	111.5	287.5	5.8	
53102-97	94	2478	0.9	0.32993	6.7	0.04612	2.1	0.31	290.6	5.9	289.5	16.8	280.5	145.4	290.6	5.9	
53102-83	200	4448	1.1	0.32308	3.7	0.04630	2.0	0.53	291.8	5.6	284.3	9.1	223.0	71.7	291.8	5.6	
53102-24	899	1422	0.6	0.35358	7.4	0.04634	4.3	0.58	292.0	12.3	307.4	19.7	425.8	135.6	292.0	12.3	
53102-69	1031	47498	1.5	0.34136	2.3	0.04697	1.0	0.44	295.9	2.9	298.2	5.8	316.5	460	295.9	2.9	
53102-92	70	2647	1.1	0.31262	15.9	0.04918	1.7	0.11	309.5	5.1	276.2	38.5	—	2.8	382.8	309.5	5.1
53102-53	650	11990	1.6	0.32729	1.7	0.05076	1.2	0.70	319.2	3.6	321.3	4.6	336.9	26.7	319.2	3.6	
53102-11	269	9235	1.0	0.37768	2.6	0.05266	1.4	0.56	330.8	4.6	325.3	7.1	286.3	48.6	330.8	4.6	
53102-14	22	4813	1.0	0.446426	2.5	0.31023	1.0	0.41	1741.8	15.5	1724.4	20.6	1703.2	41.7	1703.2	41.7	
53102-49	102	20617	1.1	0.73686	1.8	0.31872	1.2	0.64	1783.5	18.3	1773.8	15.4	1762.4	25.8	1762.4	25.8	
53102-55	249	6559	1.0	3.80783	4.0	0.25559	3.6	0.91	1467.2	47.5	1594.4	32.0	1766.8	29.9	1766.8	29.9	
53102-26	62	12896	0.9	5.24192	2.3	0.33821	1.5	0.66	1878.1	24.4	1859.5	19.5	1838.7	31.2	1838.7	31.2	
53102-71	373	81237	2.3	4.11107	8.4	0.26464	8.2	0.98	1513.5	111.0	1605.6	68.4	1842.9	27.2	1842.9	27.2	
53102-74	271	52052	1.3	4.97140	2.9	0.31787	2.3	0.80	1779.3	36.0	1814.5	24.5	1855.0	31.5	1855.0	31.5	
53102-91	153	35656	1.9	5.00957	1.5	0.31986	1.1	0.73	1789.1	16.8	1820.9	12.4	1857.6	18.1	1857.6	18.1	
53102-44	65	16175	0.8	5.36635	1.8	0.34247	1.0	0.56	1898.6	16.4	1879.5	15.2	1858.5	26.5	1858.5	26.5	
53102-81	65	13702	0.7	5.34653	2.2	0.34090	1.7	0.76	1891.0	28.1	1876.3	19.2	1860.1	26.2	1860.1	26.2	
53102-90	348	89390	1.9	5.19505	2.3	0.33116	1.2	0.55	1844.0	19.9	1851.8	19.3	1860.5	34.3	1860.5	34.3	
53102-3	148	36870	1.6	5.09617	2.3	0.32441	2.0	0.87	1811.2	31.8	1835.5	19.7	1863.1	20.6	1863.1	20.6	
53102-30	33	9611	1.1	5.28694	2.6	0.33650	1.2	0.45	1869.8	18.7	1866.8	22.1	1863.3	41.8	1863.3	41.8	
53102-93	61	17690	1.2	5.23229	1.4	0.33195	1.0	0.70	1847.8	16.1	1858.0	12.1	1869.4	18.2	1869.4	18.2	
53102-27	187	23846	1.7	5.21649	1.6	0.33080	1.3	0.78	1842.3	20.1	1855.3	13.7	1870.0	18.1	1870.0	18.1	
53102-95	298	29910	1.2	5.20592	3.3	0.34865	2.7	0.82	1928.1	45.8	1901.5	28.7	1872.6	34.1	1872.6	34.1	
53102-66	35	10883	1.4	5.38034	2.7	0.34064	1.6	0.58	1889.7	25.5	1881.7	22.8	1872.9	39.0	1872.9	39.0	
53102-102	41	9350	1.8	4.73074	2.4	0.29731	1.8	0.78	1677.9	27.1	1772.7	19.8	1886.2	26.9	1886.2	26.9	
53102-61	153	39190	1.2	5.64649	3.1	0.35400	2.9	0.95	1953.7	49.5	1923.2	26.8	1890.6	18.0	1890.6	18.0	
53102-45	59	15064	1.7	5.37392	2.5	0.33673	1.9	0.76	1870.9	30.4	1880.7	21.0	1891.5	28.6	1891.5	28.6	
53102-34	447	90369	1.3	5.50102	2.0	0.34446	1.7	0.87	1908.1	28.8	1900.8	17.3	1892.7	18.2	1892.7	18.2	
53102-62	869	156188	2.3	4.75000	2.3	0.29714	2.0	0.85	1677.1	29.3	1776.1	19.6	1894.5	22.1	1894.5	22.1	
53102-78	1706	256159	7.0	5.70934	2.3	0.35391	1.9	0.81	1953.3	31.7	1932.8	20.1	1910.9	24.4	1910.9	24.4	
53102-41	95	28725	1.0	5.35055	1.9	0.33142	1.2	0.62	1845.3	18.5	1877.0	15.9	1912.2	26.2	1912.2	26.2	
53102-2	123	19820	0.6	5.56068	4.0	0.34367	3.6	0.89	1904.3	58.7	1910.0	34.5	1916.2	33.1	1916.2	33.1	
53102-35	236	71930	1.5	5.70806	1.5	0.35269	1.0	0.68	1947.4	16.8	1932.6	12.7	1916.7	19.2	1916.7	19.2	
53102-89	457	105207	3.6	5.76906	1.9	0.35513	1.1	0.62	1959.1	19.3	1941.8	16.0	1923.4	26.2	1923.4	26.2	
53102-42	204	52652	0.4	5.66481	2.1	0.34855	1.2	0.58	1927.7	19.9	1926.0	17.7	1924.2	29.9	1924.2	29.9	
53102-13	493	101832	2.8	5.16621	3.1	0.31503	2.9	0.95	1765.4	45.3	1847.1	26.4	1940.3	17.9	1940.3	17.9	
53102-96	249	59204	1.8	5.45508	2.1	0.33464	1.5	0.73	1860.8	24.3	1893.6	17.7	1929.6	25.3	1929.6	25.3	
53102-57	860	145229	2.8	4.66567	2.3	0.28594	1.8	0.81	1621.2	26.4	1761.1	19.0	1931.3	23.6	1931.3	23.6	
53102-64	176	40618	2.1	5.68862	2.1	0.34844	1.3	0.62	1927.3	22.1	1929.6	18.5	1932.2	30.1	1932.2	30.1	
53102-67	152	54154	3.2	5.76588	2.6	0.35274	2.1	0.82	1947.7	35.8	1941.3	22.5	1934.5	26.7	1934.5	26.7	
53102-13	493	101832	2.8	5.16621	3.1	0.31503	2.9	0.95	1765.4	45.3	1847.1	26.4	1940.3	17.9	1940.3	17.9	
53102-98	82	5810	3.0	5.50412	3.0	0.33542	2.6	0.87	1864.6	42.0	1901.2	25.6	1941.5	26.3	1941.5	26.3	
53102-51	328	65004	2.7	5.94417	1.7	0.36160	1.4	0.81	1989.8	23.7	1967.7	14.9	1944.6	17.9	1944.6	17.9	
53102-10	476	17029	2.5	5.69826	4.5	0.34544	4.0	0.89	1912.8	66.6	1931.1	39.3	1950.8	37.8	1950.8	37.8	
53102-15	502	95936	1.8	5.97565	3.2	0.36219	2.0	0.62	1992.5	34.5	1972.3	28.1	1951.1	45.0	1951.1	45.0	
53102-75	112	34977	2.6	6.19617	2.6	0.37377	1.8	0.68	2047.1	30.8	2003.9	22.5	1959.6	33.6	1959.6	33.6	
53102-54	481	107778	4.6	6.01985	3.2	0.36245	2.8	0.88	1993.8	48.1	1978.7	27.9	1963.0	27.7	1963.0	27.7	
53102-104	462	87745	6.1	5.86608	3.9	0.35004	2.8	0.72	1934.8	46.7	1956.2	33.8	1979.0	48.3	1979.0	48.3	
53102-58	231	54971	1.5	5.94257	3.0	0.35208	2.7	0.91	1944.5	45.6	1967.5	25.9	1991.7	21.5	1991.7	21.5	
53102-60	651	101295	10.3	6.25415	2.6	0.37007	1.2	0.46	2029.7	20.7	2012.1	22.8	1993.9	41.3	1993.9	41.3	

Analysis	U (ppm)	206Pb	U/Th	207Pb*	Isotopic ratios				Apparent ages (Ma)				Age of youngest cluster (Ma) (3+ analyses)	
					235U (%)	238U (%)	206Pb* ±	error corr.	206Pb* (Ma)	235U (Ma)	207Pb* ±	206Pb* (Ma)		
53102-16	67	18102	1.3	5.89279	1.6	0.345587	1.2	0.77	1914.8	20.1	1960.2	13.7	2008.4	17.8
53102-38	76	19539	3.2	6.66056	2.2	0.385565	1.6	0.73	2102.6	28.8	2059.4	19.4	2016.4	26.8
53102-87	240	27937	0.4	6.46070	1.5	0.37723	1.0	0.69	2042.2	18.1	2040.6	13.2	2038.9	19.3
53102-39	672	93540	1.6	6.38039	2.0	0.36608	1.2	0.63	2010.9	21.4	2029.6	17.2	2048.6	26.9
53102-5	43	12993	7.6	6.68335	6.2	0.38017	5.5	0.89	2077.1	97.6	2070.4	54.8	2063.8	50.7
53102-47	678	132740	1.9	6.86487	1.9	0.37895	1.5	0.78	2071.4	26.0	2094.1	16.8	2116.6	20.9
53102-82	676	17942	1.0	7.07802	4.0	0.37287	3.7	0.91	2042.9	64.0	2121.3	35.7	2198.1	28.6
53102-101	368	103687	1.6	8.90521	2.2	0.42827	1.9	0.83	2297.9	35.8	2328.3	20.2	2355.1	20.8
53102-37	233	74128	1.4	8.37517	2.5	0.39458	2.3	0.92	2144.0	41.5	2272.5	22.5	2390.2	17.0
53102-32	91	29357	1.8	10.11424	2.6	0.44538	2.4	0.92	2374.7	46.8	2445.3	23.7	2504.5	16.8
53102-6	116	19240	1.3	9.95330	2.7	0.42896	2.1	0.75	2301.0	40.0	2430.5	25.4	2540.7	30.4
53102-65	796	54734	43.0	12.70687	2.6	0.51708	2.1	0.79	2686.8	45.4	2658.2	24.5	2636.5	26.2
53102-70	309	55500	4.1	10.93319	4.8	0.44255	4.1	0.85	2361.2	80.4	2517.5	44.7	2646.0	42.3
53102-23	589	81286	1.6	12.18589	4.4	0.49198	4.2	0.96	2579.2	89.7	2618.8	41.2	2649.5	20.1
53102-20	1074	34581	2.5	12.12039	2.2	0.48896	1.9	0.87	2566.2	40.6	2613.8	20.8	2650.8	18.5
53102-79	302	64450	1.5	12.40643	5.9	0.49839	5.5	0.93	2606.4	118.5	2635.7	55.9	2658.2	36.3
53102-1	31	11907	0.6	12.88653	2.7	0.51238	2.5	0.93	2666.8	55.6	2670.1	25.8	2672.5	16.6
53102-84	46	16422	0.7	13.30634	2.1	0.52644	1.2	0.54	2726.4	25.8	2701.6	20.2	2683.1	29.8
53102-4	98	24742	0.4	12.47779	2.5	0.49315	1.9	0.77	2584.3	40.5	2641.1	23.2	2684.8	26.0
53102-73	103	32250	0.9	12.47514	4.7	0.49200	3.7	0.77	2579.3	77.7	2640.9	44.5	2688.4	49.8
53102-77	96	38135	0.6	13.87382	4.5	0.53863	4.1	0.91	2777.7	93.1	2741.1	43.0	2714.3	31.3
53102-94	259	78208	1.5	13.72069	1.7	0.53172	1.0	0.59	2748.7	22.4	2730.6	16.1	2717.3	22.7
53102-110	360	94599	1.2	13.05797	2.0	0.50295	1.5	0.76	2626.4	33.1	2683.8	19.2	2727.4	21.9
53102-12	199	46612	1.5	13.65921	2.1	0.52323	1.8	0.83	2709.1	39.3	2726.4	20.3	2739.2	19.7
53102-9	136	59081	1.3	14.52497	3.7	0.55325	3.1	0.85	2838.7	71.7	2784.6	34.8	2745.7	31.6
53102-36	166	26971	1.1	14.03611	2.4	0.53301	2.1	0.86	2754.1	47.0	2752.1	23.1	2750.7	20.4
53102-7	706	43750	1.0	12.97117	9.3	0.47747	5.6	0.61	2516.2	117.0	2677.6	87.6	2801.7	120.7
53102-99	231	72870	1.5	15.31358	1.9	0.54230	1.4	0.72	2798.9	30.8	2834.9	17.9	2860.6	21.2
53102-107	190	36728	4.1	16.26024	3.3	0.54223	2.9	0.89	2792.8	66.3	2892.2	31.5	2962.2	24.2
53102-103	2418	154385	2.2	17.80254	9.3	0.53014	7.3	0.79	2742.0	163.2	2979.1	89.3	3143.3	90.6
53102-106	673	9520	1.3	19.84068	2.4	0.58529	2.2	0.91	2970.3	53.1	3083.6	23.6	3158.3	15.9

All errors are shown at the 1-sigma level, and include only measurement errors. Systematic errors (mainly from fractionation correction) add ~1% uncertainty (2-sigma) to all ages.

U concentration and U/Th have uncertainties of ~25%.

206Pb/204Pb is measured ratio.

Decay constants:  $^{235}\text{U}=1.55125 \times 10^{-10}$ ,  $^{238}\text{U}/^{235}\text{U}=137.88$ .

Isotope ratios are corrected for Pb/U fractionation by comparison with standard zircon with an age of  $564 \pm 4$  Ma (2-sigma).

Initial Pb composition interpreted from Stacey and Kramers (1975), with uncertainties of 1.0 for 206Pb/204Pb and 0.3 for 207Pb/204Pb.

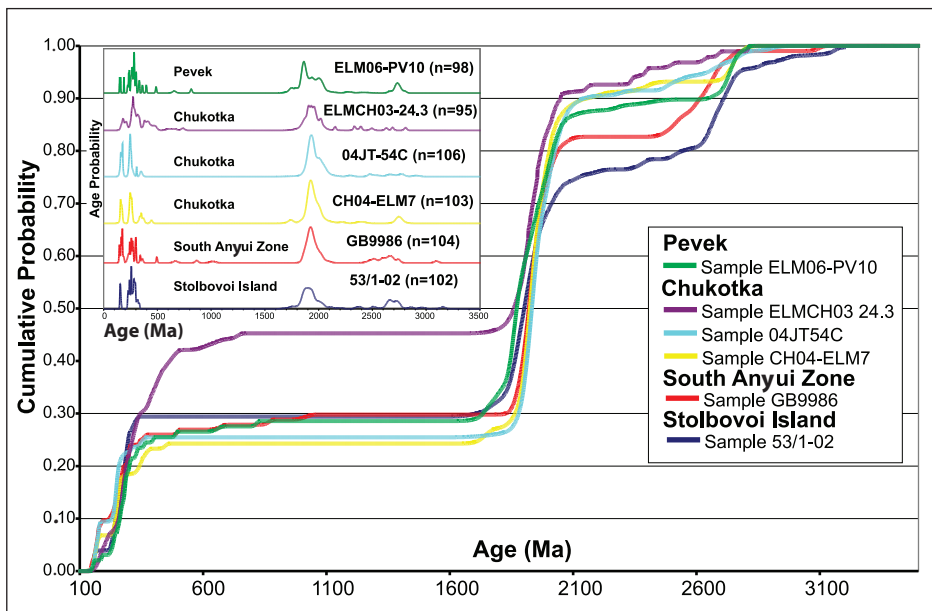


Figure 5. Cumulative age probability curves (e.g. Gehrels 2006) and relative probability distribution diagrams (inset) for detrital zircon ages.

samples (Fig. 5) and the relative age probability distribution diagrams for detrital grains younger than 1 Ga allows a more detailed comparison of the younger populations of zircons in the samples (Fig. 6).

All of the samples from Stolbovoi and Chukotka have a few Archean grains, but the age distributions have a high percentage of 2.1-1.7 Ga zircons (44-67% of the populations). This fact, together with the arkosic and mica-rich nature of the sandstones can be used to infer that Precambrian crystalline rocks were likely proximal sources for the sediments. Essentially no zircons between the ages of 1700 and 500 Ma are present in any of the samples. A second set of ages, spanning the Late Paleozoic (~320-250 Ma) is the next most abundant zircon age population. Despite the abundance of what

appear to be lithic fragments of older Triassic shales and sandstones in the Jurassic-Cretaceous deposits and the fact that Triassic strata have been found to contain zircon populations of about this age (Fig. 6, shown by grey line, from Miller et al. 2006) it is unlikely that the Late Paleozoic zircons in these rocks are mostly recycled. The reason for this is that the Triassic sediments previously studied also contain abundant Early Paleozoic zircons, which are *not* present in significant abundance in the younger Jurassic-Cretaceous strata (Fig. 6). It would be very difficult to recycle Late Paleozoic zircons from Triassic rocks into Jurassic-Cretaceous strata without also recycling some of their Early Paleozoic zircons. Based on this reasoning, we infer that Late Paleozoic magmatic rocks constituted part of the source region for Jurassic-Cretaceous sandstones. A smaller percent of detrital zircons in the Jurassic-Cretaceous sediments (~3-9%) are Jurassic in age, spanning ~175-145 Ma, with their youngest ages approaching the (fossil-dated) depositional age of the sandstones (Figs. 5 and 6, Table 3). Given the large percent of volcanic lithic fragments in the sandstones, together with the ages of detrital zircons, it seems reasonable to infer that both Late Paleozoic and Mesozoic volcanic rocks may have also been common rocks in the source regions, but likely contributed fewer zircons to the populations as compared to Precambrian gneisses and granitic rocks and Late Paleozoic and Mesozoic plutons.

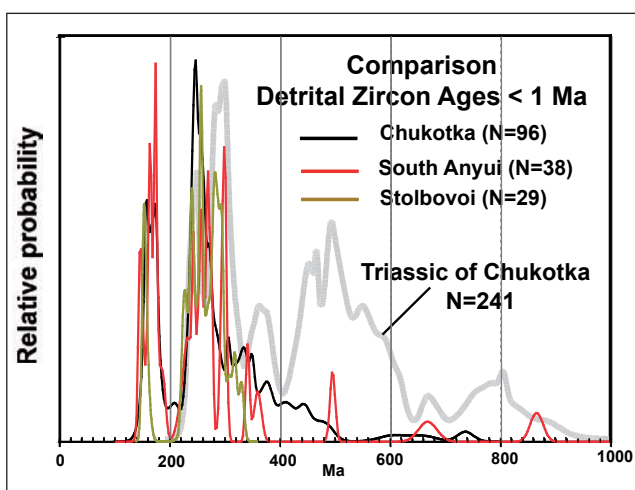


Figure 6. Comparison of detrital zircon populations younger than 1 Ga from syn-orogenic Jurassic-Cretaceous sandstones of the Russian Arctic. Light grey line represents combined data from three Triassic samples previously described from Chukotka (Miller et al. 2006; all LA-ICPMS ages, all grains < 1000 Ma, N=241).

The distributions of U-Pb detrital zircon ages in all of these sandstones are very similar to nearly identical (Figs. 5 and 6) despite the present distances between samples (Table 2). This is even more remarkable given the fact that the exact age of deposition (thus relative stratigraphic position) of the samples is not exactly known (due to lack of fossils, poor exposure, complex structure and large distances between the outcrops sampled). The high P values from the K-S test (Table

**Table 4.** K-S test results for Jurassic-Cretaceous samples from the Russian Arctic.

	K-S P-values using error in the CDF						
	53/1-02	GB9986	CH04ELM7	04JT54C	ELMCH03 24.3	ELM06-PV10	
53/1-02		<b>0.813</b>	<b>0.221</b>	<b>0.200</b>	<b>0.103</b>	<b>0.459</b>	
GB9986	<b>0.813</b>		<b>0.668</b>	<b>0.809</b>	<b>0.081</b>	<b>0.094</b>	
CH04ELM7	<b>0.221</b>	<b>0.668</b>		<b>0.999</b>	0.025	0.021	
04JT54C	<b>0.200</b>	<b>0.809</b>	<b>0.999</b>		0.010	0.006	
ELMCH03 24.3	<b>0.103</b>	<b>0.081</b>	0.025	0.010		<b>0.097</b>	
ELM06-PV10	<b>0.459</b>	<b>0.094</b>	0.021	0.006	<b>0.097</b>		

*Notes:* The K-S test is a non-parametric method for comparing cumulative probability distributions.  $P(KS)$  gives the probability that random chance alone might produce the observed difference in two distributions drawn from the same parent population. A low probability on the test, such as  $P(KS) < 0.05$ , would indicate that the differences between the two distributions are significant and that the samples are not similar in terms of their age population. If  $P(KS) >> 0.05$  then the differences are just a factor of random chance. To apply the K-S test to the data, we used the algorithm of Gynn (2006). Values that pass the K-S test at 95% confidence level and are not rejected are shown in bold letters and highlighted in yellow.

4) confirm the noted similarities between samples. ELMCH03 24.3 and ELM06 PV 10 differ the most only because of somewhat different proportions of particular age populations (Figs. 5 and 6). They have less Jurassic zircons, for instance, but are the northernmost two samples from Chukotka, and lay further from the source region during deposition. The sample from the South Anyui Zone and the one from Stolbovoi Island are remarkably similar given that they are the furthest apart today, but both represent sites that were proximal to the SAZ. Their similarities are even more remarkable considering that their petrography indicates proximal derivation, ruling out extensive reworking and/or great distances of longitudinal transport within the basin.

## Discussion of source regions for sandstones

In general, the involvement of a volcanic arc is implied in collisional models for the formation of the SAZ and the Chukotka-Anyui fold belt (e.g., Parfenov 1991; Sokolov 2002 and references therein), but the age range of magmatic activity in this arc is poorly known. Late Paleozoic intermediate to silicic volcanic sequences dated by fossils as Mississippian and Permian have been recognized in the South Anyui suture zone (Sokolov et al. 2006 and references therein). Jurassic to Early Cretaceous volcanic rocks also constitute an important structural component of the SAZ proper (the Jurassic Anyui-Svyatoi Nos island arc S of the New Siberian Islands (Kuzmichev et al. 2006)) and the Jurassic to Cretaceous Alazaya-Oloi arc of Chukotka (Dovgal 1964; Sokolov et al. 2002; Bondarenko et al. 2003). An extensive belt of granitoid plutons exists in northern Verkoyansk, south of the New Siberian Islands (Fig. 1B), called the “Main Belt” and has recently been dated by the U-Pb method utilizing the SHRIMP-RG. The intrusive history of this belt spanned the ~ 158-147 Ma time interval (Prokopiev et

al. 2007; Toro et al. 2007; Akinin et al. in press). This belt of plutons and/or silicic eruptions of this same age most likely provided the youngest zircons to the foreland basin deposits of the New Siberian Islands and the Myrgovaam-Raucha basin of Chukotka. Its location is not far from the New Siberian Islands but it lies considerably west of the Jurassic-Cretaceous deposits of Chukotka (Fig. 1A) and no major plutonic belts of this age are mapped south of the SAZ in Chukotka. There are granites mapped between the two regions that constitute what is called the “Northern Belt” but these are somewhat younger (~ 135-127 Ma, Prokopiev et al. 2007; Toro et al. 2007; Akinin et al. in press) and slightly younger than the bulk of the sedimentary succession we have studied (Tithonian to Valanginian, ~ 151-136 Ma (Gradstein et al. 2004)).

The detrital zircon age data presented here specify the age of Paleozoic and Mesozoic igneous rocks and confirms their involvement in the orogenic event that produced the Chukotka fold belt and which led to the formation of the SAZ. Both Late Paleozoic (~330-250 Ma) and Mesozoic (~175 to 145 Ma) igneous rocks are involved in the collisional event. The new data also provide better constraints on the time of closure of the South Anyui Ocean. This closure must have occurred prior to the Tithonian, when zircons were transported from southerly sources onto the AACM plate, across the SAZ. Our data further document that the orogenic highlands that shed debris into the Jurassic-Cretaceous syn-orogenic basin contained Precambrian crystalline rocks about 2.1- 1.7 Ga, an age characterizing the Siberian craton. This source region is somewhat more mysterious as there are no widespread exposures of crystalline rocks mapped directly within or south of the SAZ. However, Precambrian crystalline rocks underlie the broad Kolyma-Omolon region to the south of the SAZ (see discussion in Kolesov & Stone 2002) and are inferred to form the basement of at least part of the

Main Belt granitoids, as some of these Mesozoic plutons contain inherited Precambrian cores. (Prokopiev et al. 2007; Toro et al. 2007; Akinin et al. in press). The thrust plates that carried Precambrian crystalline rocks to the surface in order to be eroded into the Myrgovaam foreland Basin may have been subsequently buried by younger sediments.

## Discussion and conclusions

The data presented here helps establish that the New Siberian Islands and Chukotka, two distant regions, contain exposures of the same syn-orogenic foreland basin sequence, providing robust evidence for inclusion of both of these parts of Arctic Russia in the AACM as previously proposed (e.g. Parfenov & Natali'in 1985; Kuzmichev et al. 2006) (Fig. 1). However, the data present problems for the rotational opening model for the Arctic, because they further establish with greater certainty the large dimensions of this plate (Fig. 1). And certainly the Jurassic-Cretaceous match described here makes it impossible to break the plate in the center and rotate only the Chukotka part as suggested by Rowley & Lottes (1988). The discovery of Kuzmichev & Pease

(2007) that mafic dikes and sills in the New Siberian Islands link the New Siberian Islands to Siberia makes it even more difficult to rotate any part of the AACM with respect to Siberia. Our previous results tentatively linked Chukotka to NE Russia in Triassic times (Miller et al. 2006) and the new set of data presented here provides an even stronger argument for linking Chukotka to NE Russia, making it increasingly difficult to restore the AACM plate back to North America (Fig. 1B). The southerly sources documented in the syn-orogenic Jurassic-Cretaceous foreland basin sandstones could not have delivered sediment across a vast Anyui Ocean to the AACM if this ocean, or even part of it, still existed in Tithonian to Valanginian times. These relations thus tie the New Siberian Islands and Chukotka to Siberia by at least Tithonian times. Thus the Anyui Ocean must have finished closing by the latest Jurassic. These arguments make the rotational opening model for the Amerasian Basin, inferred to have taken place at a younger time 135–120 Ma (e.g., Lawver et al. 2002), increasingly difficult to champion.

To better explain the relations discussed above, we suggest an alternative hypothesis for the initial opening of the Amerasian Basin. This is depicted in simplified

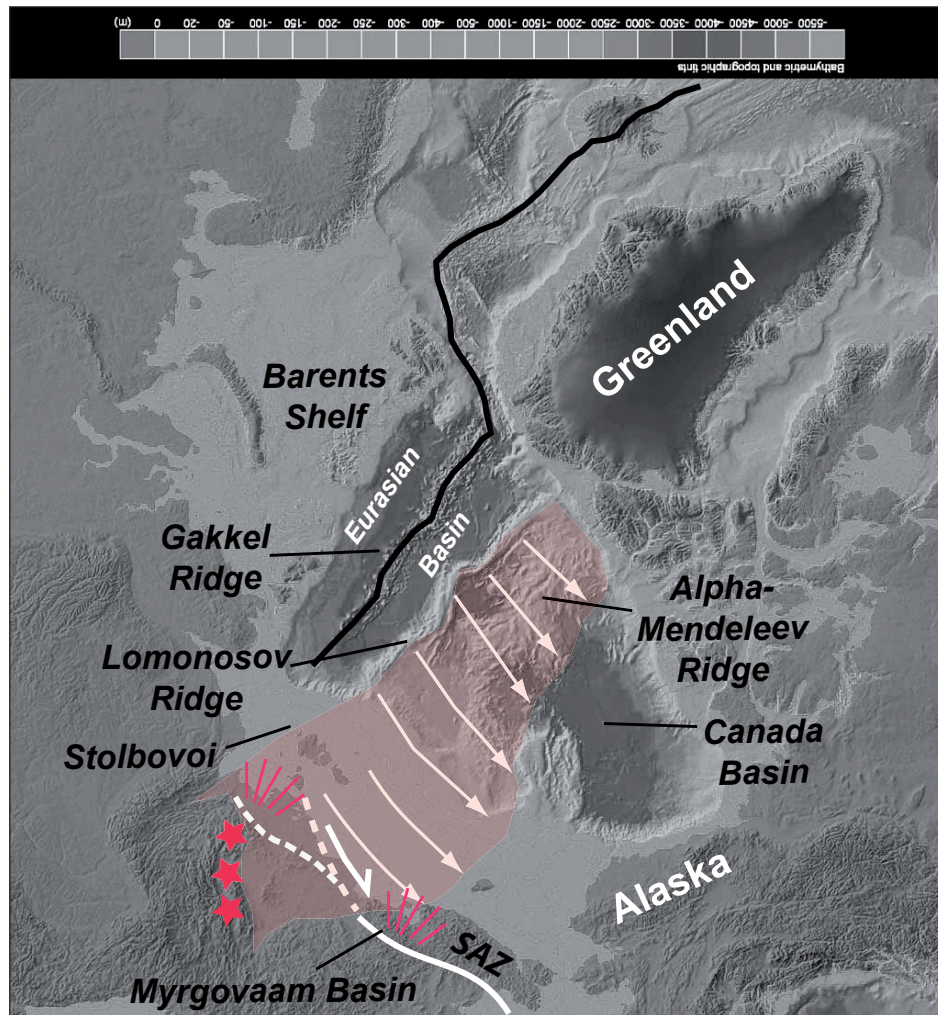


Figure 7. Speculative diagram showing a possible explanation for the separation of syn-orogenic Jurassic-Cretaceous sediments (and their identical sources) to their present positions by the rift opening of the Makarov Basin and ~100% extension of the Siberian Shelf in an E-W direction north of the SAZ. The SAZ may have operated as a transform boundary separating a more extended region to the north from a less extended one to the south. It would have also served as the locus of deformation that displaced Paleozoic and Mesozoic arc complexes southwards towards the Pacific Ocean margin.

fashion in Figure 7. The hypothesis revives previous ideas that the Makarov Basin opened by rifting in an orthogonal direction from the Lomonosov Ridge (e.g. Sweeney et al. 1982; Taylor et al. 1981; Vogt et al. 1982). The interpretation is that of the first author and is not necessarily shared by all of us (see, for instance Kuzmichev 2009, for alternative models). It by no means addresses the complete history of the formation of the Amerasian Basin, which still remains a formidable question.

The model explains the remarkable similarity in Jurassic-Cretaceous sandstones in the New Siberian Islands to those of Chukotka (as well as good matches between older geologic units (e.g. Miller et al. 2006) by the rift separation of Chukotka from the New Siberian Islands during the opening of the Makarov Basin on the Amerasian side of the Lomonosov Ridge (Fig. 7). The present separation between these two regions with identical inferred sources is explained as a function of stretching of continental lithosphere beneath both the East Siberian Shelf and the low-lying coastal region of Arctic Russia, similar to that taking place in the Laptev Sea today, south of the Gakkel mid-ocean ridge (Fig. 1A) (Drachev et al. 1998; Franke et al. 2004). The observed separation could be accommodated by ~100% extension distributed across this broad region, decreasing original distances between these exposures from ~1400 to ~700 km or less, a degree of stretching that can be anticipated in rifted and stretched continental crust and along rifted continental margins. Although there is very little data, present-day crustal thicknesses beneath the East Siberian Shelf sedimentary sequences based on a single seismic line are about 15–25 km, with an overlying sedimentary sequence up to about 8 km thick on the shelf edge (Franke et al. 2004). Since we don't know if and how much this crust was magmatically added to during rifting, original crustal thicknesses may have been only 30–50 km or so. We do know that the time of the hypothetical rifting that formed the basement to the East Siberian Shelf must post-date deposition (and deformation) of the syn-orogenic Jurassic-Cretaceous sediments described here (post 136 Ma, Gradstein et al. 2004). Widespread magmatism represented by plutons that range in age from 121 to 106 Ma in the New Siberian Islands and  $116.9 \pm 2.5$  to  $108.1 \pm 1.1$  Ma in Chukotka (Figs. 2 and 3) may be coeval with rifting as they are known to have been emplaced during E-W to NW-SE extension as documented by hundreds of dike orientations (Miller & Verzhbitsky in press).

This hypothesis (Fig. 7) would imply that the SAZ is not what it has typically been viewed as: the remains of an extensive ocean basin that closed during rotational opening of the Amerasian Basin (the Anyui Ocean in the rotational model of Lawver et al. 2002, depicted in Fig. 1B). Rather, the SAZ in this model represents parts of an allochthonous belt of oceanic and arc rocks previously thrust onto the margin of NE Russia, subsequently

slivered in a right-lateral direction along a broad, transform fault system that helped to accommodate a greater amount of extension to the north than to the south, and translated Chukotka far to the east and south (Fig. 7).

**Acknowledgements:** This project resulted from a collaborative project (Miller and Soloviev) with a visit by Soloviev to Stanford University funded by the Blaustein visiting scholar program of the School of Earth Sciences. Miller's work in Arctic Russia was supported by the American Chemical Society PRF Award 45432-AC8. Analyses of detrital zircons were funded by grants from Exxon-Mobil and Shell International. National Science Foundation EAR 0443387 (Gehrels) supports the Arizona LaserChron Center. We are indebted to Dieter Franke for an in-depth review of an earlier version of the manuscript.

## Appendix I. U-Pb geochronologic methods

U-Pb geochronology of zircons was conducted by laser ablation multicollector inductively coupled plasma mass spectrometry (LA-MC-ICPMS) at the Arizona LaserChron Center (Gehrels et al. 2006, 2008). The analyses involve ablation of zircon with a New Wave DUV193 Excimer laser (operating at a wavelength of 193 nm) using a spot diameter of 35 microns. The ablated material is carried in helium into the plasma source of a GVI Isoprobe, which is equipped with a flight tube of sufficient width that U, Th, and Pb isotopes are measured simultaneously. All measurements are made in static mode, using Faraday detectors with  $10\text{e}11$  ohm resistors for  $^{238}\text{U}$ ,  $^{232}\text{Th}$ ,  $^{208}\text{Pb}$ , and  $^{206}\text{Pb}$ , a Faraday detector with a  $10\text{e}12$  ohm resistor for  $^{207}\text{Pb}$ , and an ion-counting channel for  $^{204}\text{Pb}$ . Ion yields are ~1.0 mv per ppm. Each analysis consists of one 12-second integration on peaks with the laser off (for backgrounds), 12 one-second integrations with the laser firing, and a 30 second delay to purge the previous sample and prepare for the next analysis. The ablation pit is ~12 microns in depth.

For each analysis, the errors in determining  $^{206}\text{Pb}/^{238}\text{U}$  and  $^{206}\text{Pb}/^{204}\text{Pb}$  result in a measurement error of ~1–2% (at 2-sigma level) in the  $^{206}\text{Pb}/^{238}\text{U}$  age. The errors in measurement of  $^{206}\text{Pb}/^{207}\text{Pb}$  and  $^{206}\text{Pb}/^{204}\text{Pb}$  also result in ~1–2% (at 2-sigma level) uncertainty in age for grains that are >1.0 Ga, but are substantially larger for younger grains due to low intensity of the  $^{207}\text{Pb}$  signal. For most analyses, the cross-over in precision of  $^{206}\text{Pb}/^{238}\text{U}$  and  $^{206}\text{Pb}/^{207}\text{Pb}$  ages occurs at ~1.0 Ga.

Common Pb correction is accomplished by using the measured  $^{204}\text{Pb}$  and assuming an initial Pb composition from Stacey & Kramers (1975) (with uncertainties of 1.0 for  $^{206}\text{Pb}/^{204}\text{Pb}$  and 0.3 for  $^{207}\text{Pb}/^{204}\text{Pb}$ ). Our measurement of  $^{204}\text{Pb}$  is unaffected by the presence of  $^{204}\text{Hg}$  because backgrounds are measured on peaks (thereby subtracting any background  $^{204}\text{Hg}$  and  $^{204}\text{Pb}$ ), and because very little Hg is present in the argon gas (background  $^{204}\text{Hg}$  = ~300 CPS).

Inter-element fractionation of Pb/U is generally ~20%, whereas fractionation of Pb isotopes is generally <2%.

In-run analysis of fragments of a large zircon crystal (generally every fifth measurement) with known age of  $564 \pm 4$  Ma (2-sigma error) is used to correct for this fractionation. The uncertainty resulting from the calibration correction is generally 1-2% (2-sigma) for both  $^{206}\text{Pb}/^{207}\text{Pb}$  and  $^{206}\text{Pb}/^{238}\text{U}$  ages.

Concentrations of U and Th are calibrated relative to SRM 610 trace element glass, which contains ~460 ppm of each element. The homogeneity of this glass makes it a better concentration standard than a natural zircon crystal, and the U/Th fractionation is similar for glass and zircon.

The analytical data are reported in Table 3. Uncertainties shown in these tables are at the 1-sigma level, and include only measurement errors.

Interpreted ages are based on  $^{206}\text{Pb}/^{238}\text{U}$  for <1000 Ma grains and on  $^{206}\text{Pb}/^{207}\text{Pb}$  for >1000 Ma grains. This division at 1000 Ma results from the increasing uncertainty of  $^{206}\text{Pb}/^{238}\text{U}$  ages and the decreasing uncertainty of  $^{206}\text{Pb}/^{207}\text{Pb}$  ages as a function of age. Analyses that are >20% discordant (by comparison of  $^{206}\text{Pb}/^{238}\text{U}$  and  $^{206}\text{Pb}/^{207}\text{Pb}$  ages) or >5% reverse discordant are not included.

Cumulative and normalized relative age-probability diagrams were generated and K-S analyses were performed using routines available from [www.geo.arizona.edu/alc/](http://www.geo.arizona.edu/alc/).

## References cited

- Akinin,V.V., Prokopiev,A.V., Toro,J., Miller,E.L., Wooden,J.,Goryachev, N.A., Alshevsky,A.V., Bakharev,A.G. & d Trunilina, A.V. in press: U-Pb SHRIMP ages of granites from the Main batholith belt of the Yano-Kolyma gold bearing province. *Doklady Earth Sciences (Geochemistry)*, УДК 550.93+552.32 (571.65):549.657
- Akimenko, G.I. 2000: Geologic Map 1:200,000 scale, R-58 XXXV, XXXVI (Bilibino).
- Baranov, M.A. 1996: Nappe tectonics of the Myrgovaam Basin in North-western Central Chukotka. *Geology of the Pacific Ocean* 12, 441-448.
- Belik, G.Ya., & Sosunov, G.M., ed. 1969: Geologic map of USSR: North-Eastern Geological Directorate, Anyuisko- Chaunkskaya series, R-58-XXIX, XXX: scale 1:200,000, 1 sheet.
- Bondarenko, G.E., Soloviev, A.V., Tuchkova, M.I., Garver, J.I., & Podgornyi, I.I. 2003: Age of detrital zircons from sandstones of the Mesozoic flysch formation in the South Anyui Suture Zone (western Chukotka). *Lithology and Mineral Resources* 38, 162-176.
- Cochran, J.R., Edwards, M.H. & Coakley, B.J. 2006: Morphology and structure of the Lomonosov Ridge, Arctic Ocean. *Geochemistry, Geophysics, Geosystems* 7, Q05019, doi:10.1029/2005GC001114.
- Dovgal, Yu. M. 1964: National Geologic map of USSR, 1:200,000 scale, Anyui-Chaun Series, Sheet Q-58-IX, X, Min.Geo. Russ., Magadan.
- Dorochev, V.K. Blagoveshchensky, M.G., Smirnov, A.N. & Ushakov, V.I. 1999: New Siberian Islands. *Geologic structure and metallogeny*. VNIIOkeangeologia,130 pp. (in Russian).
- Dorochev, V.K., Malakhov, V.N., Smirnov, A.N., Ushakov, V.I., Davydov, P.S., Kryukov, V.D. & Semenov, Y.P. 2001: *Placer deposits within Lyakhovsky tin-bearing region*, St. Petersburg, VNIIOkeangeologia, 158 p., (in Russian).
- Drachev, S.S., Savostin, L.A., Grochev & Bruni, V.G. 1998: Structure and geology of the continental shelf of the Laptev sea, Eastern Russian Arctic. *Tectonophysics* 298, 357-393.
- Franke, D., Hinz, K. & Reichert, C. 2004: Geology of the East Siberian Sea, Russian Arctic from seismic images: Structures, evolution and implications for the evolution of the Arctic Ocean Basin. *Journal of Geophysical Research* 109, (B7 (B07106)), 1-19.
- Fujita, K. & Cook, D.B. 1990: The Arctic continental margin of eastern Siberia. In A. Grantz et al. (Eds.), *The Geology of North America, The Arctic Ocean Region*, 289-304, Geological Society of America, Boulder.
- Gehrels, G. (2006): Analysis Tools, <http://www.geo.arizona.edu/alc/Analysis%20Tools.htm>.
- Gehrels, G.E., Valencia, V. & Pullen, A., 2006: Detrital zircon geochronology by Laser-Ablation Multicollector ICPMS at the Arizona LaserChron Center. In Loszewski, T. & Huff, W. (Eds.), *Geochronology: Emerging Opportunities*, Paleontology Society Short Course: Paleontology Society Papers 11, 10 p.
- Gehrels, G., Valencia, V. & Ruiz, J. 2008: U-Th-Pb geochronology of zircon by Laser-Ablation Multicollector ICP Mass Spectrometry at the Arizona LaserChron Center: *Geochemistry, Geophysics, Geosystems* (in press).
- Glebovsky, V.Y., Kovacs, L.C., Maschenkov, S.P. & J.M. Brozena 2000: Joint Compilation of Russian & US Navy Aeromagnetic Data in the Central Arctic Seas. *Polarforschung* 68, 35-40.
- Gradstein, F., Ogg, J. & Smith, A. 2004: A Geologic Time Scale, Cambridge University Press, 589pp.
- Grantz, A., Eitreim, S. & Dinter, D.A. 1979: Geology and Tectonic development of the continental margin north of Alaska. *Tectonophysics* 59, 263-291.
- Grantz, A. & May, S.D. 1982: Rifting history and structural development of the continental margin north of Alaska. In J. Watkins & C. Drake (Eds.), *Studies in continental margin geology*. American Association of Petroleum Geologists Memoir, 3477-100.
- Grantz, A., May, S.D. & Hart, P.E. 1990: Geology of Arctic continental margin of Alaska. In Grantz, A., L. Johnson & J. F. Sweeney (Eds.), *The Geology of North America, v. L, The Arctic Ocean region*, 257-288, Geological Society of America, Boulder, CO.
- Grantz, A., May, S.D., Taylor, P.T. & Lawver, L.A. 1990: Canada Basin, in *The Geology of North America, v. L, The Arctic Ocean region*. In Grantz, A., L. Johnson & J. F. Sweeney (Eds.), *The Geology of North America, v. L, The Arctic Ocean region*, 379-402, Geological Society of America, Boulder, CO..
- Guynn, J. 2006: Comparison of Detrital Zircon Age Distributions Using the K-S Test, Analysis Tools, <http://www.geo.arizona.edu/alc/Analysis%20Tools.htm>
- Ivanova, N., Lebedeva, N., Zamansky, Y.Y., Langinen, A.E. & Sorokin, M.Y. 2006: Seismic profiling across the Mendeleev Ridge at 82° N: evidence of continental crust. *Geophysics Journal International* 165, 527-544.
- Katkov, S. M., Miller, E.L., Podgorny, I.I. & Toro, J. 2006: Deformation history of central Chukotka (Alarmaut Uplift) northeastern Arctic Russia. In Stone, D.B. (Ed.), *Origin of Northeastern Russia: Paleomagnetism, Geology and Tectonics*, Geophysical Institute Report UAG-R-330, University of Alaska, Fairbanks, AK (CD).
- Kolesov, E. & Stone, D.B. 2002: Paleomagnetic paleolatitudes for Upper Devonian rocks of the Omolon massif, northeastern Russia. In E. L. Miller, A. Grantz, & S. L. Klemperer (Eds.), *Tectonic Evolution of the Bering Shelf-Chukchi Sea-Arctic Margin and Adjacent Landmasses* Geological Society of America Special Paper 360, 243-258.
- Kos'ko, M.K., Bondarenko, N.S. & Nepomiluev, V.F. 1985: State geological map of the USSR, 1:200,000 scale. Sheets T-54-XXXI, XXXII, XXXIII; S-53-IV, V, VI, XI, XII; S-54-VII, VIII, IX, XIII, XIV, XV. Explanatory note, Moscow, Ministry of Geology, 162 pp. (in Russian).

- Kos'ko, M.K., Lopatin, B.G. & Ganelin, V.G. 1990: Major geological features of the islands of the East Siberian and Chukchi Seas and the northern coast of Chukotka. *Marine Geology* 93, 349-367.
- Kuzmichev, A.B. 2009: Where does the South Anyui suture go in the New Siberian Islands and Laptev Sea?: Implications for the Amerasian Basin origin. *Tectonophysics*, doi: 463, 86-108/j.tecto.2008.09.017.
- Kuzmichev, A.B. & Lebedev, V.A. 2008: On the age of oceanic basalts on Big Lyakhov Island (New Siberian archipelago): Outlining the western edge of Jurassic South Anyui Ocean. *Doklady (Transactions) of Russian Academy of Sciences*, 421A, 884-888.
- Kuzmichev, A.B. & Pease, V.L. 2007: Siberian trap magmatism on the New Siberian Islands: constraints for Arctic Mesozoic plate tectonic reconstructions. *Journal Geological Society London* 164, 959-968.
- Kuzmichev, A.B., Sklyarov, E.V. & Barash, I.G. 2005: Pillow basalts and blueschists on Bol'shoi Lyakhovsky Island (the New Siberian Islands)-fragments of the South Anyui oceanic lithosphere. *Russian Geology and Geophysics* 46, 1367-1381.
- Kuzmichev, A. B., Soloviev, A. V., Gonikberg, V. E., Shapiro, M. N. & Zamzhitskii, O. V. 2006: Mesozoic Syn-collision siliciclastic Sediments of the Bol'shoi Lyakhov Island (New Siberian Islands). *Stratigraphy and Geological Correlation* 14, 30-48.
- Lawver, L. A., Grantz, A. & Gahagan, L.M. 2002: Plate kinematic evolution of the present Arctic region since the Ordovician. In Miller, E.L., Grantz, a. & Klempner, S.L. (Eds.), *Tectonic Evolution of the Bering Shelf-Chukchi Sea-Arctic Margin and Adjacent Landmasses*. Geological Society of America Special Paper 360, 333-358.
- Lawver, L. A. & Scotese, C.R. 1990: A review of tectonic models for the evolution of the Canada Basin. In Plafker, G. & H. C. Berg (Eds.), *The geology of North America, v. G-1, The Geology of Alaska*. Geological Society of America, Boulder, CO, 49-140.
- Layer, P.W., Newberry, R., Fujita, D., Parfenov, L., Trunilina, V. & Bakharev, A. 2001: Tectonic setting of the plutonic belts of Yakutia, northeast Russia, based on 40Ar/39Ar geochronology and trace element geochemistry. *Geology* 29, 167-170.
- Ludwig, K. R. 2003: User's manual for Isoplot 3.0: A geochronological toolkit for Microsoft Excel, Special Publication 4, 71 pp., Berkeley Geochronol. Center, Berkeley, Calif.
- MacNab, R. 2006: Developing outer continental shelf limits in the Arctic Ocean: Geoscience encounters UNCLOS Article 76. In, Scott, R.A. & Thurston, D.K. (Eds.), Proceedings of the Fourth International Conference on Arctic Margins, U.S. Dept. of Interior, Minerals Management Service, Anchorage, AK, p. 189-198.
- Miller, E.L., Katkov, S.M., Strickland, A., Toro, J., Akinin, V.V. & Dumitru, T.A. (in press): Geochronology and thermochronology of Cretaceous plutons and metamorphic country rocks, Anyui-Chukotka fold belt, North East Arctic Russia. In .B. Stone et al. (Eds.), *Origin of Northeastern Russia: Paleomagnetism, Geology and Tectonics*, EGU Stephan Mueller Publication Series.
- Miller, E.L., Toro, J., Gehrels, G., Amato, J.M., Prokopiev, A., Tuchkova, M.I., Akinin, V.V., Dumitru, T.A., Moore, T.E., & Cecile, M.P. 2006a: New Insights into Arctic paleogeography and tectonics from U-Pb detrital zircon geochronology. *Tectonics* 25, TC3013, doi: 10.1029/2005TC001830.
- Miller, E.L., Toro, J., Gehrels, G., Tuchkova, M., Katkov, S., 2006b: Detrital zircon ages from Late Jurassic-Early Cretaceous Myrgovaam Basin sandstones (Rauchua Trough), western Chukotka, NE Russia. In Stone, D.B. (Ed.), *Origin of Northeastern Russia: Paleomagnetism, Geology and Tectonics*, Geophysical Institute Report UAG-R-330, University of Alaska, Fairbanks, AK (available as CD).
- Miller, E.L., & Verzhbitsky,V. In press: Structural Studies in the Pevek region, Russia: Implications for the evolution of the East Siberian Shelf and Makarov Basin of the Arctic Ocean. In D.B. Stone et al. (Eds.), *Origin of Northeastern Russia: Paleomagnetism, Geology and Tectonics*, EGU Stephan Mueller Publication Series.
- Mutti, E., Tinterri, R., Benevelli, G., Biase, D. & Cavanna, G. 2003: Deltaic, mixed and turbidite sedimentation of ancient foreland basins. *Marine and Petroleum Geology* 20, 733-755.
- Nokleberg, W.J. & others, 1994: Circum-North Pacific tectono-stratigraphic terrane map: U.S. Geological Survey Open File Report 94-714, 433 p., 2 sheets, scale 1:5,000,000, 2 sheets scale 1:10,000,000.
- Nokleberg, W.J., Parfenov, L.M., Monger, J.W.H., Norton, I.O., Khanchuk, A.I., Stone, D.B., Scholl, D. W. & Fujita, K. 1998: Phanerozoic Tectonic Evolution of the Circum-North Pacific, U.S. Geological Survey Open File Report 98-754, 126p.
- Paraketsov, K.V. & Paraketsova, G.I. 1989: *Stratigraphy and fauna of Upper Jurassic and Lower Cretaceous deposits in northeast USSR*. Moscow, Nedva, 297pp.
- Parfenov, L.M. 1991: Tectonics of the Verkhoyansk-Kolyma Mesozoids in the context of plate tectonics. *Tectonophysics* 199, 319-342.
- Parfenov, L.M., & Natalin, B.A. 1986: Mesozoic tectonic evolution of northeastern Asia. *Tectonophysics* 127, 291-304.
- Prokopiev, A.V., Toro, J., Miller, E.L., Wooden, J., Trunilina, V.A. & Bakharev, A.G., 2007: Granitoids of the Main batholith belt (NE Asia): New U-Pb SHRIMP geochronological and geochemical data. In A. I. Khanchuk (Ed.), *Tectonics and metallogeny of the Circum-North Pacific and Easternmost Asia*. Proceedings of the Leonid Parfenov Memorial Conference, Khabarovsk, FEBRAS p. 286-288.
- Rowley, D.B. & Lottes, A. L. 1988: Plate-kinematic reconstructions of the North Atlantic and Arctic: Late Jurassic to Present. *Tectonophysics* 155, 73-120.
- Samusin, A.I. & Belousov, K.N. 1985: State Geological Map of the USSR, scale 1:200,000. New Siberian Island Series. Sheets S-53-XVI, XVII, XXIII; S-54-XIV-XVI, XX-XXVII, XXVII-XXX, Explanatory notes by A.M. Ivanova. Soyuzgeofond, Moscow, 130 pp. (in Russian).
- Sekretov, S.B. 2001: Northwestern margin of the East Siberian Sea, Russian Arctic: seismic stratigraphy, structure of the sedimentary cover and some remarks on the tectonic history. *Tectonophysics* 339, 353-383.
- Sokolov, S.D., Bondarenko, G.Ye., Morozov, O. L., Shekhovtsov, V.A., Glotov, S.P., Ganelin, A.V., Kravchenko, B. & Berezhny, I.R. 2002: South Anyui suture, Northeast Arctic Russia; facts and problems. In E.L. Miller, A. Grantz & S.L. Klempner (Eds.), *Tectonic Evolution of the Bering Shelf-Chukchi Sea-Arctic Margin and Adjacent Landmasses*. Special Paper of the Geological Society of America 360, 209-224.
- Sokolov, S.D., Bondarenko, G.E., Tuchkova, M.I., & Layer, P. 2006: Tectonic position and origin of volcanosedimentary rocks of the Polyarnyi Uplift (South Anyui Suture, western Chukotka), *Doklady Earth Sciences* 411, 1199-1203.
- Sosunov, G.M., & Tiliman, S.M., ed. 1960: Geologic map of USSR: North-Eastern Geological Directorate, Anyuisko- Chaunskaya series, R-58-XXXV, XXXVI: scale 1:200,000, 1 sheet.
- Stacey, J.S., & Kramers, J.D. 1975: Approximation of terrestrial lead isotope evolution by a two stage model. *Earth and Planetary Science Letters* 26, 207-221.
- Sweeney, J.F.,Weber, J.R., & Blasco, S.M. 1982: Continental ridges in the Arctic Ocean: LOREX constraints. *Tectonophysics* 89, 217-238.
- Taylor, P.T., Kovacs, L.C.,Vogt P.R. & Johnson, G.L. 1981: Detailed aeromagnetic investigations of the Arctic Basin. *Journal of Geophysical Research* 86, 6323-6333.
- Toro, J., Prokopiev, A.V., Miller, E.L., Trunilina, V.A. & Bakharev, A.G. 2007: Origin of the main granitoid belt of northeastern Russia on the basis of new U-Pb geochronology and geochemistry. Fifth International Conference on the Arctic Margins, Abstracts and Proceedings, Geological Society of Norway, Tromsø, Norway, Abst. # 10-057, 73-74.
- Vogt, P.R., Kovacs, L.C., Bernero, C. & Srivastava, S.P. 1982: Asymmetric geophysical signatures in the Greenland-Norwegian and southern Labrador Seas and Eurasian Basin. *Tectonophysics* 89,

- 95-160.  
Vol'nov, D.A., Ivanenko, G.V., Kos'ko, M.K. & Lopatin, B.G. 1998: State Geological Map of the Russian Federation, scale 1:1,000,000(New Series) Sheet S-53-55-New Siberian Islands, VSEGEI, St. Petersburg (in Russian).